



**HAL**  
open science

# Converting carbon vulnerable lands to wood plantations for use as building materials: overall environmental performance and time-dependent assessment of carbon dioxide removals

Zhou Shen, Lorie Hamelin, Ligia Tiruta-Barna

## ► To cite this version:

Zhou Shen, Lorie Hamelin, Ligia Tiruta-Barna. Converting carbon vulnerable lands to wood plantations for use as building materials: overall environmental performance and time-dependent assessment of carbon dioxide removals. *Journal of Cleaner Production*, 2023, 388, pp.136040. 10.1016/j.jclepro.2023.136040 . hal-04335081

**HAL Id: hal-04335081**

**<https://hal.science/hal-04335081>**

Submitted on 11 Dec 2023

**HAL** is a multi-disciplinary open access archive for the deposit and dissemination of scientific research documents, whether they are published or not. The documents may come from teaching and research institutions in France or abroad, or from public or private research centers.

L'archive ouverte pluridisciplinaire **HAL**, est destinée au dépôt et à la diffusion de documents scientifiques de niveau recherche, publiés ou non, émanant des établissements d'enseignement et de recherche français ou étrangers, des laboratoires publics ou privés.

1 **Converting carbon vulnerable lands to wood plantations for use as building materials:**  
2 **overall environmental performance and time-dependent assessment of carbon dioxide**  
3 **removals.**

4

5 Zhou Shen, Lorie Hamelin, Ligia Tiruta-Barna\*

6 TBI, Université de Toulouse, CNRS, INRAE, INSA, Toulouse, France

7 \* corresponding author

9 **Abstract**

10 Bioeconomy addresses the triple balancing challenge posed by the Paris Agreement: inducing  
11 additional GHG mitigation alongside biophysical carbon dioxide removals, while keeping fossil  
12 carbon in the ground. The use of woody plants as construction materials could simultaneously  
13 address this challenge: CO<sub>2</sub> is absorbed through photosynthesis, while wood-based products  
14 provide mitigation by replacing either petrochemical materials such as plastic boards or energy-  
15 intensive materials like bricks. This study combines, at the scale of France, static and dynamic  
16 life cycle assessment with soil carbon simulations to investigate the long-term environmental  
17 performance of using, as input for the building sector, black locust (*Robinia pseudoacacia* L.)  
18 planted on “carbon vulnerable lands”. These are areas specifically selected for their low soil  
19 organic carbon (SOC) levels and low potential to interfere with food security. After the  
20 consecutive cultivation of three rotations, black locust was shown to stock an additional 92000  
21 kg ha<sup>-1</sup> of carbon in soils as SOC. The mitigation effect from the plastic board replacement is  
22 the major contributor to the assessed environmental impacts, including climate change, leading  
23 the black locust system to generally perform better than the reference system where the carbon  
24 vulnerable areas are left as they are with their initial vegetation. Considering that cultivation  
25 starts in 2022, the dynamic evaluation of the global mean temperature change (GMTC) shows  
26 that the black locust system results in net negative emissions in the near- and mid-term, but  
27 with a GMTC overshoot in the second half of the century. Even if a considerable carbon stock is  
28 created through time (e.g., 81% and 39% of the carbon captured by photosynthesis, in 2050 and  
29 2100 respectively), the GHG emissions stemming from manufacturing and end-of-life  
30 processes were shown to offset the benefit of carbon capture.

32 **Keywords:** soil organic carbon, consequential life cycle assessment, dynamic life cycle  
33 assessment, climate change mitigation, biomass, negative emissions

34

35 **Graphical abstract (see figures document)**

36

37

38

39

40 **Highlights:**

- 41 • Black locust plantation and utilization in buildings induce negative emissions
- 42 • Black locust system yields greater climate benefits than the initial vegetation
- 43 • Plastic board replacement explains the superior performance for 13/16 impacts
- 44 • By 2136, the largest temperature reduction of  $3.9E-09$  K per ha is simulated
- 45 • 15% of the carbon captured by 3 rotations is still stocked after 260 years

46

47

48 **List of Abbreviations**

49

50 A radiative efficiency of a GHG

51 B atmospheric burden of a GHG

52 BL black locust scenario

53 BLc black locust scenario evaluated by consequential LCA

54 BLa black locust scenario evaluated by attributional LCA

55 C carbon

56 CLT cross-laminated timber

57 CO<sub>2</sub> carbon dioxide

58 CSAAP carbon Storage in Arable land and Anthropogenic Products

59 CV-land carbon vulnerable land

60 FU functional unit

61 g emission flow of a GHG

62 GHG greenhouse gas

63 GMTC global mean temperature change

64 iLUC indirect land use change

65 IRF concentration - impulse response function of a GHG

66 IRFT temperature – impulse response function

67 LCA life cycle assessment

68 MDF medium density fiberboard

69 REF reference scenario

70 REFc reference scenario evaluated by consequential LCA

71 REFa reference scenario evaluated by attributional LCA

72 RF radiative forcing

73 SOC soil organic carbon

74 SM supplement information material

75 t metric ton

76 y year

77

78

79

80

81

## 82 **1. Introduction**

83 Achieving the climate objectives of the Paris Agreement and national policies in terms  
84 of emissions reduction and carbon neutrality by 2050 implies the implementation of drastic  
85 greenhouse gas (GHG) emission reductions and carbon dioxide (CO<sub>2</sub>) capture and storage  
86 actions. To this end, the concept of Carbon Storage in Arable land and Anthropogenic Products  
87 (CSAAP) has recently been proposed (Shen et al., 2022b), consisting in cultivating plants, also  
88 called biopumps, that can induce a net increase of soil organic carbon (SOC) stocks while  
89 providing biomass for long-lasting anthropogenic products.

90 Putting CSAAP into practice needs solving two issues, namely defining the type of  
91 suitable biopump species and areas to grow them. According to previous research (Shen et al.,  
92 2022b), there are up to 2,400,000 ha of suitable land in France alone that could be available for  
93 planting biopumps for climate mitigation purposes. These lands are called ‘carbon vulnerable  
94 lands (CV-lands)’ as they present a high potential for SOC sequestration due to their current  
95 SOC stock being <50 t C ha<sup>-1</sup> (Minasny et al., 2017). They were also selected to respect a set  
96 of specific sustainability criteria defined in Shen et al. (2022b). Among the list of 14 suitable  
97 woody biopumps presented in Shen et al.(2022b), black locust (*Robinia pseudoacacia* L.) was  
98 highlighted not only because it could capture 31.5 kg CO<sub>2</sub> per tree per year (Supplementary  
99 material, SM, section 2.1), but also for its capacity to convert part of the captured C in the soil  
100 as SOC (Wang et al., 2012). Furthermore, woody products have a relatively long lifetime, hence

101 delaying the return of C to atmosphere as gaseous emissions (CO<sub>2</sub>, and eventually methane and  
102 carbon monoxide) .

103         When analyzing how wood value chains affect climate change, the conventional theory  
104 considers biogenic CO<sub>2</sub> as neutral (balanced), thus neither CO<sub>2</sub> absorbed nor CO<sub>2</sub> emitted from  
105 biomass is included in climate change impact calculations (Chen et al., 2019; da Costa et al.,  
106 2018). This approach is suitable for annual or short rotation coppice, while not proper in  
107 estimating forest mitigation potential because the effect of C storage and delayed emission is  
108 ignored. Guest et al. (2013) studied the relationship between the wood rotation and C storage  
109 in products on the biogenic global warming potential. They concluded that in order to consider  
110 biogenic CO<sub>2</sub> as neutral, the lifespan of wood products should be at least half of the plantation  
111 rotation. Another common accounting approach is considering the forest as a permanent C sink,  
112 where the CO<sub>2</sub> captured through photosynthesis is counted while the emission of biogenic CO<sub>2</sub>  
113 is not (González-García et al., 2011). This approach shows the effectiveness of biomass as a C  
114 sink on a limited time scale, however, it is not correct under time scales encompassing the life  
115 cycle of biomass from cradle-to-grave. Albers et al. (2019b) modeled the trees' growth and  
116 residue decomposition, showing that the tree's lifetime highly influences the mitigation  
117 potential, the shorter the lifetime, the lower the mitigation effect of converting forests to  
118 biofuels. However, since biofuels are used at once with almost all C emitted immediately, there  
119 is no technosphere C sink. Lan et al. (2020) tracked the carbon flows from one rotation of pine  
120 forest cultivation to the end of wood products on a 100-year scale, and highlighted the  
121 difference between using residue for wood products or energy. They treated biogenic CO<sub>2</sub> as  
122 neutral, only considering the influence of fossil CO<sub>2</sub> emissions. Zieger et al. (2020) counted  
123 both biogenic CO<sub>2</sub> absorption by timber and wheat, and degradation of biobased walls including  
124 incineration and compost, in a time-dependant manner. However, the belowground part of  
125 plants and the SOC changes were not included in these studies. Soil is an important C sink, not

126 taking it into account results in C flows that are not correctly balanced (Hamelin et al., 2012).  
127 Moreover, because aerial crops are commonly harvested, soil and root carbon storage is a key  
128 determinant of climate change mitigation potential, and tends to be higher with greater plant  
129 diversity, according to experimental results (Yang and Tilman, 2020).

130         The most existing LCA studies use a static approach and CO<sub>2</sub>-eq as an aggregation  
131 metric for all GHG, independently of the time scale considered, which could mislead the  
132 conclusions (Barna, 2021; Saez de Bikuña et al., 2018; Zieger et al., 2020). Because wood and  
133 wood-based products have a relatively long lifespan, and biomass residues decay at different  
134 rates, the temporal factor is essential in assessing wood product systems. Recent studies  
135 demonstrated a considerable difference between static and dynamic LCA approaches for wood-  
136 based products (e.g., Cardellini et al., 2018; Göswein et al., 2020), especially for the  
137 quantification of biogenic CO<sub>2</sub> capture and release effects. A recent study pointed out that for  
138 woody products, the static LCA overestimates the long-term cumulative impact without  
139 providing information on short-term impact (Cordier et al., 2022). Although the study built the  
140 results on a temporal inventory of C flows, the climate change impact was calculated by a metric  
141 based on CO<sub>2</sub>-eq which induces a bias in the results.

142         This work explores the mitigation potential for global warming and for overall  
143 environmental impacts, of an application case of the CSAAP strategy with perennial plantations,  
144 selected in the light of earlier work (Shen Zhou; Ligia Tiruta-Barna Shivesh Kishore Karan;  
145 Lorie Hamelin, 2022). The case is the implementation of a 35-y plantation of black locust on  
146 CV-lands in France, using the biomass for bio-based products intended for the building sector.  
147 Objectives are to: 1) evaluate the C sinks induced over time, 2) investigate the overall  
148 environmental consequences of replacing current CV-land and fossil-based products with the  
149 black locust system and the related bio-based products, and particularly the global warming  
150 mitigation potential in order to contrast it with the sinks, and 3) investigate the effect on global

151 mean temperature change in time. In the general endeavor to uncover environmentally-  
152 performant solutions towards both carbon dioxide removals and GHG mitigation, this work  
153 proposes an original, comprehensive framework with adapted modeling tools to address all  
154 these objectives, and to fill gaps in the existing literature. The C flows were modeled from the  
155 tree cultivation to products manufacturing and end of life (for a cradle-to-grave scope), and the  
156 C pools in soil (SOC) and materials (biomass) were estimated in function of time. The time  
157 period encompasses the tree cultivation (three rotations) but also the product lifetime and end  
158 of life period with slow material degradation. The dynamic C balance, but also all GHG  
159 temporal emissions over the life cycle were integrated in dynamic LCA for global warming  
160 impact, evaluated by the global mean temperature change indicator. The overall environmental  
161 consequences of changing the initial land use to black locust cultivation and utilization were  
162 evaluated with the consequential LCA approach. Finally, sensitivity and uncertainty analysis  
163 were performed to explore the robustness of the results obtained.

164

165

## 166 **2. Methods**

### 167 **2.1. Scenarios description**

168 The point of departure of this analysis is one hectare of average French CV-land, to be  
169 either converted for black locust cultivation from the year 2022, over three rotations of 35-y  
170 each (BL Scenario), or maintained as CV-land for 105 y (reference scenario, from here onwards  
171 referred to as REF Scenario). For the static environmental assessment, only 35 years (the time  
172 of one rotation) is considered, as further detailed in section 2.5.

173

#### 174 **2.1.1 Initial vegetation scenario on CV-land (REF Scenario)**

175 This scenario considers that CV-lands remain CV-lands throughout the time covered by  
176 the analysis. The vegetation considered on average French CV-land stem from the work of  
177 (Shen et al., 2022; Shen Zhou; Ligia Tiruta-Barna Shivesh Kishore Karan; Lorie Hamelin,  
178 2022). Accordingly, four types of initial land cover are considered with different shares in terms  
179 of the area they cover, namely intensive grasslands (53%), natural grasslands (20%), rapeseed  
180 lands (20%), and woody moorlands (7%) (details in Shen et al., 2022b). Ryegrass (*Lolium*  
181 *perenne* L.) and rapeseed (*Brassica napus* L.) represent the initial vegetation on intensive  
182 grassland and rapeseed lands, respectively, while heather (*Calluna vulgaris*) is selected to  
183 represent both natural grasslands and woody moorlands vegetation. On CV-lands remaining  
184 CV-lands, ryegrass and rapeseed are harvested annually and used for animal feed and oil  
185 production respectively, while heather is considered to decay on-site (Pehme et al., 2017). The  
186 rapeseed cake co-produced with rapeseed oil is also considered to be used for animal feed.

187

### 188 **2.1.2 Black locust scenario (BL)**

189 In this scenario, CV-lands are ploughed prior to black locust planting. Black locust is a  
190 nitrogen-fixing species and tolerates droughts (Nicolescu et al., 2020; Seserman et al., 2018).  
191 For this reason, and also in accordance with the CSAAP vision to favor systems with minimal  
192 inputs (Shen et al., 2022), no fertilization or irrigation is considered. To remove defective trees,  
193 selective thinning is conducted twice, in the 10<sup>th</sup> year and 20<sup>th</sup> year of the plantation's lifetime,  
194 where whole trees are removed (Keresztesi, 1983; Nicolescu et al., 2020). After the second  
195 selective thinning, extra branches are pruned to provide enough space for stem growth. After  
196 harvesting, black locust is delimbed and debarked. Barks are incinerated to provide heat for  
197 downstream manufacture (Silva et al., 2013), while branches are chopped into wood chips (Fig.  
198 1a). Stumps are crushed and left on the ground as residues during thinning operations when  
199 black locust is logged.

200           The processes after logging are depicted in Fig. 1b. First, there is the processing of stems.  
201   After delimiting and debarking, the stems are dried on open fields to meet a moisture content  
202   of ca. 15% (Żelazna et al., 2019). The dried stems are trimmed and sawn into panels, then  
203   laminated into several layers (Sahoo et al., 2019). These high-value laminated panels, called  
204   ‘cross-laminated timber’ (CLT), are widely used in the building sector, as a more sustainable  
205   alternative than carbon-intensive materials (Cadorel and Crawford, 2019; Cowie et al., 2021).  
206   Herein CLT is assumed to be used for exterior walls, with 50 years lifespan (Dodoo et al., 2014).  
207   After demolition, 45% of CLT is incinerated, 45% is recycled, while the remaining 10% is lost  
208   (regarded as open-landfills) (Jayalath et al., 2020). The recycled CLT is chopped into wood  
209   chips for further treatment.

210           Second, the branches from stem’s trimming are cut into chips (to produce medium  
211   density fiberboard, MDF), then wood chips are washed to remove the dust. The clean chips are  
212   mixed with other wood chips obtained from branches, along with the woody material from 1<sup>st</sup>  
213   and 2<sup>nd</sup> thinning and recycled CLT. All these materials are softened in a steam-pressurized  
214   digester (the heat to generate steam commonly comes from burning barks), then mixed with  
215   urea-formaldehyde resin and additives in the resonating process, to improve the strength  
216   (Puettmann et al., 2016). The mixture is pressed into boards (MDF) at 170 °C for ca. 5 minutes  
217   using a mechanically controlled oil-heated press (Yuan and Guo, 2017). The produced MDF  
218   has multiple usages. Having a lower mechanical strength than CLT, it is more suitable for  
219   furniture and interior architecture (Piekarski et al., 2017). After 12 years of use, most MDF in  
220   Europe is incinerated with heat recovery, while a minor part is landfilled (Courret et al., 2017;  
221   ecoinvent, 2020). The scraps occurring through the MDF production process are considered to  
222   end in open-landfills.

223

224 Fig. 1 Process flow diagram showing the key activities considered for (a) black locust  
225 cultivation, harvesting (green) and residual biomass management (orange), and (b) manufacture  
226 and disposal of cross-laminated timber (CLT; yellow) and medium density fiberboard (MDF;  
227 blue).

228

## 229 **2.2. Overview of the methodology used**

230 The methodology used to achieve the objectives of this study builds on material and  
231 energy flow calculation, encompassing all stages from plant cultivation to anthropogenic  
232 production and products' end of life, to finally evaluate the carbon pools and environmental  
233 impacts.

234

235 Fig. 2 Calculation steps followed in this study

236

237 As shown in Fig. 2, the first step calculates the growth of black locust to determine how  
238 much CO<sub>2</sub> is captured by photosynthesis, how much biomass is produced in function of time in  
239 the different parts of the plant (e.g., belowground, aboveground), and the quantity of residues  
240 destined to decay above- and below ground. The carbon in the residues is an input to a SOC  
241 model, whose evolution is simulated over the rotation time span. In this way, the yearly content  
242 of SOC is estimated (over 105 years), along with the CO<sub>2</sub> releases from mineralization or native  
243 SOC losses, as detailed in section 2.4. The harvested biomass enters the manufacturing chains  
244 and determines the amount of products, associated by-products, and all related flows in the  
245 process chain, from harvesting to product manufacturing and end of life. Data from literature  
246 have been used to model the material and energy balances for the manufacturing processes.

247 These foreground flows are then used in three different LCA modeling approaches to  
248 respond to different questions as later detailed: static consequential LCA, dynamic LCA using

249 the same consequential modeling of the inventory, and dynamic LCA using the attributional  
250 modelling of the background inventory with system expansion in the foreground part. For the  
251 dynamic approaches, the material and energy flows have been used as time series with their  
252 time occurrence depending on the system's timeline. Both dynamic approaches used temporal  
253 predictions for electricity mix (used in the background inventory) based on either the absolute  
254 values or the rate of changes.

255

### 256 **2.3 Black locust growth rate**

257 Black locust is a fast-growing tree species. After seedling planting, it reaches its fastest  
258 growth rate at year 20, then the growth rate slows down gradually till the end of the rotation  
259 (year 35) (Ciccarese et al., 2014; Nicolescu et al., 2018). The volume of biomass is estimated  
260 from the height and diameter at breast height, calculated in function of time (Rédei et al., 2014,  
261 2012). The wood volume is converted to biomass dry matter considering a wood density of 785  
262 kg m<sup>-3</sup> DM (Adamopoulos et al., 2007) (SM 2.2).

263 The whole stand is assumed to grow at the same rate, thus the below-ground biomass is  
264 calculated based on a fixed shoot/ root ratio in time, here taken to 1.73 (Chen et al., 2020). In  
265 order to calculate the biomass amount per ha in a specific year, a density varying between 560–  
266 2240 trees per ha is considered, according to the growth stage (Keresztesi, 1983; Nicolescu et  
267 al., 2018). Details and results of simulated annual biomass partition (above- and below ground;  
268 in standing biomass and residues; as woody and non-woody portions) are presented in SM 2.2.

269 The foliage, pods, and seeds are considered jointly under the umbrella term 'aerial  
270 biomass', and are regarded as an annual input to soils from the 6<sup>th</sup> year of the rotation (Stone,  
271 2009; Warne, 2016). Similar to the root biomass, the aerial biomass increase in time with the  
272 tree growth (Ciccarese et al., 2014). It was estimated based on a fixed ratio (1.2% of wood  
273 biomass, DM).

274

## 275 **2.4 Simulating SOC on CV-lands for both scenarios, and wood residues decay**

276 The evolution of SOC on CV-lands cultivated with black locust or covered with initial  
277 vegetation was simulated with C-TOOL (Taghizadeh-Toosi et al., 2014). This model was  
278 adopted as one of the few models easily usable (i) with unconventional (non-agricultural) crops,  
279 (ii) for perennial systems, and (iii) calibrated for temperate areas (Andrade et al., 2022). Among  
280 others, it has the advantage that the proportion of C incorporated in the different (virtual) soil  
281 pools (each with a different turnover rate affected by clay content and temperature; C-TOOL  
282 considers three pools) is easily customizable (e.g., Hansen et al., 2020). This ease of  
283 customization also applies to the allometric equations used to define the proportion of  
284 aboveground residual biomass input to the soil annually. Different applications of the model  
285 with perennial crops include (Hamelin et al., 2012) and (Keel et al., 2017).

286 The simulation was conducted with a one-year time step, for a timespan of 105 years  
287 from 2022 to 2126, corresponding to three consecutive rotations of black locust. Meteorological  
288 conditions in France were predicted by SICLIMA (DRIAS CERFACS, IPSL, last updated May  
289 2013) for the RCP4.5 climate trajectory (Representative Concentration Pathway; Chen et al.,  
290 2021), downscaled by the model CNRM-CERFACS-CM5/CNRM-ALADIN63. In C-TOOL,  
291 only the monthly average temperature is required in terms of meteorological data input (Fig.  
292 s1). The required soil characteristics include the soil clay content and the C/N ratio. The former  
293 was retrieved from the same database used for identifying CV-lands (GSOC; Food and  
294 Agriculture Organization of the United Nations, 2020), the latter, not included in GSOC, was  
295 set to 11 based on relevant literature (Clivot et al., 2019; Launay et al., 2021). The average  
296 initial SOC content for the CV-lands was evaluated as 42350 kg SOC ha<sup>-1</sup> (Shen et al., 2022).

297 Finally, one other key input required by the model is the annual C input from residual  
298 above- and belowground biomass. The aboveground residues includes aerial biomass (foliage,  
299 seeds, and pods), which fall down annually (except for the first five years), and stumps, which

300 are crushed and left on the ground as residues during thinning operations and when black locust  
301 is logged (year 10<sup>th</sup>, 20<sup>th</sup>, 35<sup>th</sup> of the rotation, respectively). Belowground residues consist of  
302 decaying roots and rhizodeposits. Decomposition rate coefficients of 0.12, 0.008, and 0.003  
303 months<sup>-1</sup> were set for aerial, aboveground- and belowground wood biomass, respectively  
304 (Taghizadeh-Toosi et al., 2014). To represent the slower decay of woody above- and below-  
305 ground residues, the simulation was conducted for an additional 100 years after the last rotation  
306 (the C not emitted after 100 years is considered as permanently stored).

307 For the initial vegetation, consisting of four different land types, the SOC of each land  
308 type was simulated individually, then aggregated together based on their respective shares in 1  
309 ha CV-land (C input in Table s19). A decomposition rate coefficient of 0.12 month<sup>-1</sup> was used  
310 for the initial vegetation' residual biomass inputs to soil (above- and below-ground), as used  
311 for the foliage and as used in e.g., Hamelin et al. (2012) and Taghizadeh-Toosi et al. (2014)  
312 (both on the basis of Petersen et al., 2005).

313

## 314 **2.5 Environmental impact assessment through consequential LCA**

### 315 **2.5.1 Goal, boundary, and functional unit**

316 Consequential LCA is used to evaluate the environmental consequences of (i)  
317 cultivating black locust instead of the initial vegetation on the identified CV-lands in France  
318 and (ii) using the biomass in anthropogenic products while replacing conventional (fossil-based)  
319 products. This implies that multifunctionality was modeled with system expansion (Fig. 3) and  
320 that the life cycle inventories for marginal suppliers were considered. The functional unit is  
321 defined as 'using 1 ha of CV-land in France for cultivating perennial crops over one full rotation,  
322 and using the harvestable biomass within the bioeconomy'. For the scenarios considered herein,  
323 this implies 35 years. The LCA framework follows the ISO 14040 and 14044 standards (ISO,

324 2006a, 2006b). The system boundary considered for the consequential LCA is shown in Fig. 3,  
325 both for the BL (here BLc) and REF (here REFc) scenarios.

326

327 Fig. 3 System diagrams showing the boundaries considered in consequential LCA of business  
328 as usual (REFc) and black locust (BLc) systems, built on REF and BL scenarios respectively.

329 CV-land: carbon vulnerable land; iLUC: Indirect land use changes; CLT: cross-laminated  
330 timber; MDF: medium density fiberboard. Full lines indicate induced processes while dotted  
331 lines represent avoided processes.

332

333 System BLc involves a variety of substitutions. The vegetable oil (rapeseed oil) and feed  
334 (ryegrass silage, rapeseed cake), no longer reaching markets because CV-lands are now used  
335 for black locust have to be compensated for (Saez de Bikuña et al., 2018). This may happen  
336 through two main reactions, namely expansion of nature for agriculture (deforestation) or  
337 intensification of agricultural land (Tonini et al., 2016), both considered herein under the  
338 umbrella term of indirect land use changes (iLUC). According to market reports and literature  
339 review, the bio-based CLT and MDF will replace light-clay bricks and polyvinyl-chloride  
340 boards (herein referenced as plastic boards), respectively (Onyeaju et al., 2012; Takano et al.,  
341 2014). Incineration, at all stages where it happens, is considered with heat recovery, which  
342 implies that this heat will not need to be generated the way it would have otherwise been. As a  
343 result, corresponding heat generation is avoided. Finally, the use of CLT at the expense of bricks  
344 (replaced material) was considered to lead to a 52% reduction of the electricity consumed in  
345 the erection and demolition phases, because of the lighter mass (Corradini et al., 2019; Guo et  
346 al., 2017).

347

## 348 **2.5.2 Life cycle inventory**

349 Life cycle inventories for foreground processes (Fig. 1) were established on the basis of  
350 literature, models, and a variety of estimation proxies when necessary. These are  
351 comprehensively detailed in the SM (Tables s3-s18). The displaced feed service (for the silage  
352 ryegrass and rapeseed cake of the initial vegetation) and its substitution by corresponding  
353 marginal carbohydrates, protein and lipid ingredients, along with the associated land use  
354 changes were modelled according to the methodology described in (Tonini et al., 2016).  
355 Landfilling processes (open-landfilling and landfilling of MDF at the end-of-life) were  
356 modelled according to the model provided in IPCC (2019), which proposes a time-dependant  
357 decay function, and that C emissions arise as 14% CH<sub>4</sub>-C, and 86% CO<sub>2</sub>-C. According to the  
358 IPCC (2019) landfilling model, 15% of the products' biogenic C is considered to end as  
359 emissions to air. For the static LCA, the overall SOC change simulated with C-TOOL was, for  
360 both systems (BLc and REFc), annualized (i.e. distributed equally) over the 35 years of the  
361 rotation. All the background inventories were taken from Ecoinvent v3.5 (ecoinvent, 2020),  
362 with the consequential model.

363

### 364 **2.5.3 Life cycle impact assessment and interpretation**

365 The environmental impact assessment was performed with the Environmental Footprint  
366 method (EF) recommended by European Commission (Fazio et al., 2018a). Moreover, because  
367 all CO<sub>2</sub> releases and adsorption are accounted, biogenic CO<sub>2</sub> was considered with a global  
368 warming potential of 1 kg of CO<sub>2</sub>-eq per kg biogenic CO<sub>2</sub> instead of the value of 0 used in  
369 (Fazio et al., 2018a).

370 For interpretation, a contribution analysis was performed for each impact category,  
371 where processes with negative and positive contributions were analyzed separately in two  
372 groups. In each group, the processes contributing to at least 80% of the impact were selected  
373 for further in-depth analysis, i.e., identifying their sub-processes and substances contributing to

374 the impact (Fazio et al., 2018b). The LCA was facilitated with the SimaPro software, version  
375 9.1.

376

## 377 **2.6 Dynamic LCA for evaluating climate change impact**

378 Given the long lifetime of the studied system, a time-dependent method is necessary to  
379 address the temporal dimension of the climate change impact. Dynamic LCA with the global  
380 mean temperature change (GMTC) as an indicator was applied herein. The method and  
381 computational tool used were presented in previous works (Tiruta-Barna, 2021; CCI-tool, 2021).  
382 The GMTC calculation used the recommended method of IPCC, for the emission timing over  
383 the whole life cycle of scenarios (Stocker et al., 2013), for all GHGs included in the ecoinvent  
384 v3.5 database (Table s21), and can be summarized by the following main equations.

385 The atmospheric burden of substance  $s$ ,  $B_s$  (kg), is calculated as the convolution product  
386 (symbol  $*$ ) between the temporal emissions of the substance,  $g_s$  (kg.year<sup>-1</sup>), and the  
387 concentration - impulse response function of that substance,  $IRF_s$  :

$$388 B_s(t) = g_s * IRF_s = \int_0^t g_s(t') IRF_s(t - t') dt' \quad (1)$$

389 where  $t$  and  $t'$  are two time scales. The radiative forcing RF is calculated by:

$$390 RF_s(t) = A_s(t) B_s(t) = A_s(t)(g_s * IRF_s) \quad (1)$$

391 where  $A_s$  (W.m<sup>-2</sup>.kg<sup>-1</sup>) is the radiative efficiency (considered as constant). IRF and  $A$  are  
392 specific for each GHG (Stocker et al., 2013). The global mean temperature change generated  
393 by the forcer  $s$  is defined as the convolution product between its RF and the temperature impulse  
394 response function IRFT:

$$395 GMTC_s(t) = RF_s * IRFT_s \quad (3)$$

396 IRFT is independent of the type of GHG. The mean temperature change at a given time  $t$ ,  
397 GMTC (K), is obtained by aggregating values for all the concerned forcers:

$$398 \text{GMTC}(t) = \sum_s \text{GMTC}_s(t) \quad (4)$$

399  
400 In scenario BL, trees are cultivated on 1 ha of land for three consecutive rotations, from  
401 2022 to 2126. The same time span is considered for the initial vegetation lasting on the CV-  
402 lands in scenario REF. The temporal inventory (limited herein to GHGs) was obtained by  
403 placing each process on the timeline shown in Fig. 4. For long-lasting biogenic GHG emissions  
404 (e.g., those stemming from the disposal of CLT and MDF), the longest emission time was set  
405 as 100 years because the C released after 100 years can be considered permanently stored  
406 (European Commission-Joint Research Centre., 2010). Therefore, the temporal scope spans  
407 over the implantation of the first rotation in 2022, up to the end of the emissions, in 2290, from  
408 the last MDF disposal, covering 267 years in total. The manufacturing processes were  
409 considered to occur in the year of biomass harvesting. The time step for the inventory  
410 calculation was set to 1 year, regarded as sufficiently fine for climate change impact calculation.

411 Two perspectives were adopted for the dynamic modeling, here referred to  
412 ‘consequential’ and ‘attributional’, despite not fully embracing all features attributed to these  
413 two types of modeling approaches (Brandao et al., 2017; Schaubroeck et al., 2021). These two  
414 perspectives imply two main differences. One is the system boundary, as illustrated in Fig. 3  
415 for the consequential perspective and Fig.5 for the attributional perspective. Both perspectives  
416 compare the black locust system to a reference situation. In the consequential perspective, the  
417 system expansion reactions (associated with both the products generated in the BL system and  
418 the consequences of the foregone use of CV-land) are placed in the BL system (or here BLc).  
419 Even the foregone use of CV-land (emissions associated with growing ryegrass, rapeseed, and  
420 heather) could have been placed in this system for an entirely relative perspective, it was left as

421 a reference (here REF<sub>c</sub>) for comparison purposes. Two realities are compared in what is here  
422 referred to as “attributional perspective”. In one (BL<sub>a</sub>), black locust is grown on CV-land and  
423 used to produce heat, CLT, MDF (the latter two being in use for a number of years and disposed  
424 of at their end-of-life, the same way as in the BL<sub>c</sub> system), while vegetable oil is supplied by  
425 palm oil and feed by marginal feed ingredients. In the other system (REF<sub>a</sub>), CV-land is used as  
426 CV-land, but to make it equivalent, the alternatives to products generated in the BL<sub>a</sub> system  
427 (heat, bricks, plastic boards) are considered here. Strictly speaking, these two system boundaries  
428 are equivalent (and would typically be both labelled as “consequential”). The major difference  
429 between the two perspectives lies in the type of background data being used. The consequential  
430 perspective considered marginal data, e.g., those foreseen to react to a demand change in the  
431 long-term (concretely translating in the use of the so-called consequential background  
432 processes), while the attributional perspective used average background data (cut-off processes).  
433 Moreover, for the foreground data requiring heat and electricity, the attributional perspective  
434 considered the mix composition predictions made for France for different periods (2020-2030,  
435 2030-2040, 2040-2050), based on Kassara et al. (2019) for electricity and (ADEME, 2018) for  
436 heat. The heat and electricity mixes after 2050 were considered the same as in 2050 (Table s22-  
437 24). For the consequential perspective, the marginal French electricity mix of Ecoinvent v3.5  
438 was considered (2050; based on predictions from (European Commission, 2021)). For  
439 foreground heat, natural gas is considered.

440

441 Fig. 4 Timeline of processes for dynamic LCA.

442

443 Fig. 5 System diagrams of business as usual (REF<sub>a</sub>) and black locust (BL<sub>a</sub>) systems, built on  
444 REF and BL scenarios respectively.

445

## 446 **2.7 Sensitivity and uncertainty analysis**

447 To explore the robustness of the obtained results and identify the hotspots, sensitivity  
448 and uncertainty analysis were conducted for both scenario BLc and REFc. The method and  
449 results are described in SM 5 and 6, for the sensitivity and uncertainty of the systems,  
450 respectively.

451

## 452 **3 Results and discussion**

### 453 **3.1 Black locust growth and decay**

454 Based on simulated height and diameter (Fig. s5), the biomass amount on 1 ha CV-land  
455 is shown in Fig. 6a, in different parts of black locust. During each thinning operation (year 10  
456 and 20), half of the tree (in terms of dry matter, DM) is logged, in year 10 and 20, producing  
457 26 and 110 t of woody DM respectively, being further chipped to produce MDF. The final  
458 harvesting at year 35 produces 368 t DM of stem (which is used to produce CLT), and 136 t  
459 DM of branches used for MDF. Based on the different turnover rate simulated by C-TOOL, 10%  
460 and 27% of the DM in above- and belowground wood residues is still undegraded after 35 years.  
461 This falls to 1.5% and 2.8% after 100 years of decomposition.

462

### 463 **3.2 SOC simulation results**

464 The simulation results with C-TOOL (Fig. 6b) shows that SOC increased at the end of  
465 the rotation with black locust while slightly decreased with the initial vegetation. The black  
466 locust induces a SOC increase periodically with each rotation, reaching 92040 kg ha<sup>-1</sup> at the  
467 end of the third rotation (year 2126). The greatest increase is observed during the first rotation  
468 with 73650 kg ha<sup>-1</sup>. The SOC increase is less important for the subsequent rotations, being only  
469 15540 and 2840 kg ha<sup>-1</sup> for the second and third rotation respectively, since the SOC gradually

470 reaches saturation in soils (Petersen et al., 2013). Declining SOC stocks are observed following  
471 every biomass removal event (harvest, thinning) due to lesser input into the soil.

472 Unlike the black locust system, the SOC in the initial vegetation system decreased from  
473 42350 to 40680 kg ha<sup>-1</sup> during the cultivation (105 years). The main difference between black  
474 locust and initial vegetation is the C input. According to the literature data for vegetation yield  
475 and to the simulation results for black locust growth, the aboveground C inputs from initial  
476 vegetation is higher than that from black locust aerial biomass (foliage, seeds and pods) (1.27  
477 and 0.91 t ha<sup>-1</sup> year<sup>-1</sup> respectively). The higher C input implies that a greater quantity of C is  
478 humified; as a result, the SOC of the initial vegetation is higher than black locust until year  
479 2031. But at years 10, 20, and 35 of the rotation, there are extra C inputs from logged stems,  
480 especially from the belowground root portion (below-ground: 4.65, 19.23, 65.24 t C ha<sup>-1</sup> from  
481 the first-, second thinning, and harvesting respectively), making the SOC of the black locust  
482 system being higher than the one of the initial vegetation. Meanwhile, compared to the initial  
483 vegetation residues, the gradual decomposition of black locust residues keep the C in the soils  
484 for a longer time, leading to the SOC of black locust exceeding the SOC of the initial vegetation  
485 system by year 2041 (second thinning).

486

487 Fig. 6 Simulated (a) biomass growth and decay for black locust during one rotation, and (b)

488 SOC evolution for black locust and initial vegetation during the cultivation period.

489 Harvestable biomass: stem, branch and bark.

490

491 Considering the 105 years studied herein, an annual SOC increase of 880 kg ha<sup>-1</sup> is  
492 observed for the black locust system, corresponding to an increase rate of 21‰ per year, which  
493 can be compared to the 4‰ target reported by Minasny et al. (2017) to offset the global annual  
494 GHG emissions. Looking at each rotation in isolation, this yearly increase rate is 50‰ during

495 the first rotation and 30‰ during the first-two rotations, indicating that short-term cultivation  
496 might be more efficient. Ciccarese et al. (2014) simulated one rotation of black locust with the  
497 Yasso model, and observed an annual SOC increase of 110 kg ha<sup>-1</sup> year<sup>-1</sup> before the final  
498 harvest which is half of our result (220 kg ha<sup>-1</sup> year<sup>-1</sup> for the first rotation). On the other hand,  
499 Wang et al. (2015) reported, based on field measurements, an average annual SOC increase of  
500 930 kg ha<sup>-1</sup> (over 25 years). They measured this increase to 2200 kg ha<sup>-1</sup> annually from year 5-  
501 10 but only 290 kg ha<sup>-1</sup> from year 10-25. Both studies also highlighted the contribution of dead  
502 wood incorporated in soils.

503 It should be noticed that the high SOC at the end of harvesting does not last for a long  
504 time. Fig. s2 shows that following the last stem harvest, the SOC decreases gradually since  
505 there is no extra C input anymore. After 51 years (2177) and under the conservative assumption  
506 that the soil is left bare, all SOC gained with the black locust cultivation is lost, the SOC stock  
507 being equivalent to the initial level of 2022.

508

### 509 **3.3 Environmental impact results from the static LCA**

510 The LCA results are shown in Fig. 7 (climate impact; global warming potential for a  
511 100-y time horizon, GWP<sub>100</sub>) and Fig. 8 (all other impacts); the negative contributions represent  
512 avoided processes or emissions while positive contributions represent the processes induced by  
513 implementing the studied scenario. The difference between these represents the net impact of a  
514 given category and scenario. Results are expressed per functional unit.

515

#### 516 **3.3.1 Climate change**

517 Both scenarios lead to a negative characterized impact for climate change, but  
518 scenario BLc leads to a larger magnitude than scenario REFc (-2202 vs -51 t CO<sub>2</sub>-eq). In  
519 scenario BLc (Fig. 1a), the tree cultivation and the avoided plastic boards processes shape the

520 net negative score, respectively contributing with -1283 and -2509 t CO<sub>2</sub>-eq. The material  
521 substitution contributes the most to negative results, which is also observed in a recent LCA  
522 study on woody products (Cordier et al., 2022). The avoided plastic board process is an  
523 aggregation of several activities. About 61% of its impact is due to petrochemical plastic  
524 manufacture, while 24% stems from incineration at the end-of-life (Fig. s4). The negative score  
525 of tree cultivation reflects the net 1305 t CO<sub>2</sub> captured by black locust in one rotation, offsetting  
526 the positive GHG emission due to the iLUC in the same process (21 t CO<sub>2</sub>-eq).

527 On the other hand, emissions during the biomass logging (combining harvesting,  
528 thinning and pruning processes), and the disposal of MDF products are the main positive  
529 contributors, with similar magnitudes. For logging, the GHG emission comes from the residue  
530 decomposition, with 68% due to CO<sub>2</sub> and 26% due to CH<sub>4</sub>. For the product disposal, since 45%  
531 of CLT is recycled to produce MDF at the end of life, the disposal of MDF plays a more critical  
532 role (MDF: 545 vs CLT: 139 t CO<sub>2</sub>-eq emitted). The important contribution of MDF disposal  
533 to climate change is due to the CO<sub>2</sub> emitted during the incineration (mainly comes from the  
534 woody part).

535 Fig.7 Climate change impact for (a) BLc and (b) REFc. Processes with contributions lower than  
536 1% of the total impact (in absolute) were attributed to categories others (+) or (-) (Process  
537 contributions were computed as follows: e.g., process A has a contribution of 1 and process B  
538 of -1, then the contribution of process A is  $1/(abs(1)+abs(-1))=50%$ ; details in SM). FU:  
539 functional unit.

540

541 For scenario REFc (Fig. 7b), natural grasslands and woody moorlands are shown as net  
542 contributors to the climate change impact. This reflects the emissions of CH<sub>4</sub> and N<sub>2</sub>O due to  
543 the on-site decomposition of residues. Intensive grasslands and rapeseed lands contribute to the  
544 total negative score with 68% and 32% respectively, which in both cases is essentially due to

545 the avoided marginal vegetable oil (from rapeseed oil production) and marginal feed (from  
546 rapeseed meal and silage production). Based on the results of section 3.2 (increase of 92040 kg  
547 SOC ha<sup>-1</sup> in 105 y), planting black locust increases, in average over the course of one rotation,  
548 the CV-lands SOC by an amount equivalent to 112 t CO<sub>2</sub>-eq, while maintaining the initial  
549 vegetation leads to SOC decreases corresponding to 2 t CO<sub>2</sub>-eq. Compared to the net results of  
550 the two scenarios, the effect of the C change in soils is relatively small, representing 5% and 4%  
551 of the net scores in scenario BLc and REFc, respectively.

552

### 553 3.3.2 Other environmental impacts

554 All impact results except climate change are presented in Fig. 8. Among all fifteen  
555 environmental impacts of Fig. 8, there are four and twelve with a net positive score for scenario  
556 BLc and REFc, respectively (Table 1, in red). Comparing scenario BLc to REFc, cultivating  
557 black locust instead of the initial vegetation benefits all environmental impacts except ionizing  
558 radiation, freshwater eutrophication, and land use.

559

560 Table 1. Summary of the impact results. Positive impact values on grey background. BLc is  
561 better than REFc for the impacts highlighted in italic bolds.

Impact	Unit	BLc	REFc
Climate change	kg CO2 eq	<i>-2202407</i>	-51061
Ozone depletion	kg CFC11 eq	<i>-0.034</i>	0.00488
Ionising radiation, HH	kBq U-235 eq	<i>9937</i>	1847
Photochemical ozone formation, HH	kg NMVOC eq	<i>-8217</i>	478
Respiratory inorganics	disease inc.	<i>-0.39</i>	0.030
Non-cancer human health effects	CTUh	<i>-0.17</i>	0.26
Cancer human health effects	CTUh	<i>-0.049</i>	0.0022
Acidification terrestrial and freshwater	mol H <sup>+</sup> eq	<i>-4137</i>	4616
Eutrophication freshwater	kg P eq	<i>407</i>	-11.2
Eutrophication marine	kg N eq	<i>-1318</i>	883

Eutrophication terrestrial	mol N eq	-13252	21422
Ecotoxicity freshwater	CTUe	-3767847	-1002667
Land use	Pt	26884194	15617187
Water scarcity	m3 depriv.	-8296011	-460070
Resource use, energy carriers	MJ	-45018209	263511
Resource use, mineral and metals	kg Sb eq	0.25	1.49

562

563            Similar to climate change, avoided conventional products is the main contributor to the  
564 negative impact in scenario BLc. This particularly applies for plastic boards, especially due to  
565 the suspension polymerization operation (Fig. s6). However, the avoided use of plastic boards  
566 does not consistently translates with negative impacts. Without their incineration at the end-of-  
567 life, extra heat and electricity production are induced in the BLc system. Hence, avoiding the  
568 disposal of plastic boards generates burdens in ionizing radiation, freshwater eutrophication,  
569 and land use, representing 13%, 81%, and 46% of the positive scores, respectively. It also  
570 explained why in these three impacts, scenario BLc is worse than scenario REFc. In addition,  
571 in land use impact, rapeseed and silage ryegrass avoid palm oil and animal feed and the related  
572 necessary land, which reinforce this result.

573            In the scenario BLc, positive impact contributions come from multiple source across the  
574 different impacts, but agricultural management and products manufacturing tend to be two key  
575 contributors. The major agricultural management activities are tree logging processes (first- and  
576 second thinning, pruning, and harvesting). The diesel used in machines for logging and skidding  
577 trees to open-dry is the primary contributor, with some exceptions (e.g. PM<sub>10</sub> from dust being  
578 the main contributor for respiratory inorganics). Since there is no fertilizer and pesticide use,  
579 the influence of black locust cultivation is negligible except in land use. Nevertheless, the  
580 agricultural activities during the cultivation (like the chemical application and diesel used for  
581 agricultural machines) are the main impact sources in scenario REFc, as observed in the LCA  
582 of common crops (Silva et al., 2014).

583 As widely admitted in woody board production (Piekarski et al., 2017; Yuan and Guo,  
584 2017), the resin (urea-formaldehyde resin here) used as additive is the main positive score  
585 contributor (47%) in the manufacture chain, especially in mineral resource use. Furthermore,  
586 free formaldehyde emitted from the cure of urea-formaldehyde resin is another potential pitfall,  
587 causing more than half (56%) of positive score in cancer human health impact. Therefore,  
588 increasing the use of cellulosic materials in the fiberboard production for avoiding the resin use  
589 can be an efficient pathway to reduce the environmental impacts (Puettmann et al., 2016).

590

591 Fig. 8 LCA results for BLc (left bar) and REFc (right bar) scenarios for all impact categories  
592 of the EF method, with the exception of climate change.

593

### 594 **3.4 Dynamic LCA results**

#### 595 **3.4.1 Dynamic LCA in consequential modelling**

596 GMTC results for the whole 269 years period considered (timeline in Fig. 4) are  
597 presented in Fig. 9. In the result analysis, distinction is made between the GHG (and related  
598 GMTC) stemming from the biomass (growth, decay, utilization, and end of life), noted as “bio”,  
599 and the other GHGs coming from anthropogenic processes referenced as “non-bio” (despite  
600 stemming from biogenic processes like e.g., iLUC). The GMTC indicator has the property of  
601 additivity, thus the ‘total’ GMTC is the sum of GMTC from bio and non-bio contributors.

602 Concerning the REFc scenario, the GMTC (Total REFc; red curve) is positive during  
603 the cultivation period (up to 2126) except the first five years due to the avoided products. During  
604 the cultivation, 76% of captured CO<sub>2</sub> is released in a short time from the residue decomposition.  
605 Moreover, 3% of the C emitted by anaerobic decomposition of residues is as CH<sub>4</sub>, in the first ten  
606 years (2022-2031). The contribution of CH<sub>4</sub> represents up to 25% of REFc’s bio GMTC, but  
607 this contribution decreases sharply (due to the short life time of CH<sub>4</sub> in atmosphere), shortly

608 after the last cultivation period, leading to the decrease of bio GMTC from 2131 onwards.  
609 Meanwhile, non-bio GMTC decreases continuously because the main contributor is the avoided  
610 CO<sub>2</sub> from the replaced feedstock, a long-live GHG, thus with long term effect. The short  
611 lifespan of biogenic CH<sub>4</sub> and the relatively long-term CO<sub>2</sub> emissions from non-bio sources lead  
612 the non-bio GHG to dominate the trend of scenario REFc after the year 2150.

613

614 Fig. 9 GMTC results for all GHG sources from REFc and BLc scenarios, and the  
615 consequence of replacing REFc with BLc (Net GMTC). Total BLc = Bio BLc + Non bio  
616 BLc; Total REFc = Bio REFc + Non bio REFc; Net GMTC = Total BLc – Total REFc. 1<sup>st</sup>,  
617 2<sup>nd</sup>, 3<sup>rd</sup> refer to the rotation number.

618

619 For the BLc scenario, in the first years of cultivation, the CO<sub>2</sub> captured is low and SOC  
620 mineralization is relatively high (Fig. 6b), making the bio GMTC slightly positive (Fig.9, Bio  
621 BLc). The BLc GMTC becomes negative in year 2028 (Fig. 9, Total BLc), reflecting, among  
622 others, the carbon captured in both biomass and as SOC as the black locust stand grows. The  
623 CH<sub>4</sub> contribution to bio GMTC represents a maximum of 9%, CO<sub>2</sub> being the largest contributor.  
624 The increase of bio GMTC (Bio BLc) after the last rotation is explained by the end of CO<sub>2</sub>  
625 capture, and the bio GHG emissions from the end of life incineration of MDF and CLT (the  
626 stored biogenic C is released back to the atmosphere).

627 The GMTC of non-bio sources (Non-bio BLc) is positive at the beginning, due to the  
628 emissions from tree plantation and iLUC. After the second thinning (year 2041), non-bio  
629 GMTC becomes negative, and between 2042 and 2047, closely follow the GMTC of bio BLc.  
630 However, from 2048 onwards, bio and non-bio GMTC drastically change paths, with non-bio  
631 GMTC importantly decreasing due to the plastic boards and bricks replacement by the bio-  
632 based products (MDF and CLT), involving manufacturing, use, and end-of-life processes. The

633 biggest GHG contributor is the avoided CO<sub>2</sub> emission from the plastic board life cycle. The  
634 avoided plastic boards are counted at the time when MDF is produced, namely during first and  
635 second thinning, harvesting, and CLT recycling (years 2032/2067/2102, 2042/2077/2112,  
636 2057/2092/2127, 2108/2142/2178 respectively). The sharp decrease around 2057 is due to more  
637 plastic boards being avoided by more MDF being produced at the final harvest.

638 The net GMTC is negative just 5 years after the start of the first rotation, revealing that  
639 replacing the scenario REF<sub>c</sub> by BL<sub>c</sub> can mitigate global warming from the 5<sup>th</sup> year onwards.  
640 The mitigation effectiveness increases with the cultivation duration, with a peak around year  
641 2136 (i.e. 10 years after the end of the last rotation), with a temperature reduction of -3.94E-09  
642 K by ha of black locust cultivation. A minor part of the net negative GMTC is due to the bio  
643 flows, and reflect the higher CO<sub>2</sub> absorption of black locust compared to the initial vegetation.  
644 However, it is the non-bio GHG flows of BL<sub>c</sub>, and hence the avoided materials, that essentially  
645 determine the net GMTC result (Fig.9).

646

### 647 **3.4.2 Dynamic LCA in attributional modeling**

648 The GMTC results for the attributional perspective ( average background processes with  
649 system expansion) are presented in Fig. 10, for REF<sub>a</sub> (top) and BL<sub>c</sub> (bottom) scenarios. The  
650 impact of each system is referenced as “net” REF<sub>a</sub> and BL<sub>c</sub>, obtained by the aggregation of all  
651 system’s contributors. In this modeling approach, only the CO<sub>2</sub> capture processes result in  
652 negative GMTC, all other processes generate impacts, hence positive GMTC.

653 In REF<sub>a</sub> system, the bio REF<sub>a</sub> is the same as the bio REF<sub>c</sub>, and will accordingly not be  
654 further detailed. In the first decades, the impacts of agricultural management and later activities  
655 (Non-bio REF<sub>a</sub>), involving oil mill operation and ryegrass silage, are negligible compared to  
656 the GMTC from biogenic GHG flows. In REF<sub>a</sub> system, the biggest contributor is the plastic  
657 board (production, use, and end-of-life incineration), dominating the net REF<sub>a</sub> after 2043. CO<sub>2</sub>

658 and CH<sub>4</sub>, emitted as pulse in the years of MDF manufacture and disposal, are the primary  
659 contributors to GMTC, while conventional brick and heat production contribute little to the net  
660 GMTC result. The REFa system, despite its slightly negative net GMTC during the first years,  
661 is, as for REFc, shown as inadequate for global warming mitigation.

662 The net GMTC of the BLa system is negative in short and mid term with an overshoot in  
663 the second halph of the century. Albeit very few studies exist combining carbon flows of the  
664 whole life cycle of the plant with dynamic GMTC evaluation, this kind of behavior with  
665 negative and positive domains was observed for other wood-based building materials (Negishi  
666 et al., 2019). The bio contributor of BLa scenario is the same as in consequential modeling and  
667 was analyzed in section 3.4.1. The non-bio GHG emissions stem from iLUC, wood logging  
668 operation, MDF&CLT production, disposal processes, and all related background processes,  
669 and always lead to positive GMTC. The GMTC from non-bio sources increases continuously,  
670 with sharp slopes when impulse emissions occur from these processes. At the end of  
671 anthropogenic activities, non-bio GMTC remains at a highe level for long term due to the  
672 accumulation of CO<sub>2</sub> (long lived gas) emitted during the whole time span. Because the CO<sub>2</sub>  
673 capture vanishes with the harvesting of wood, the net GMTC increases and becomes positive  
674 in 2072, then decreases sharply with the tree growth during the second rotation. Following the  
675 same trend, after the second rotation, the GMTC becomes positive for a while and continues to  
676 increase due to the non-bio contributors and additional processes. Concerning the additional  
677 products, induced feed ingredients affect the GMTC more than palm oil, CO<sub>2</sub> emission during  
678 the agricultural management being the major contributor.

679  
680 Fig. 10. GMTC evolution in REFa (above) and BLa (bottom) scenario with time. 1<sup>st</sup>, 2<sup>nd</sup>, 3<sup>rd</sup>  
681 refer to the rotation number. Total BLa = Bio BLa + Non bio BLa; Net BLa = Total BLa +

682 Palm oil + Feed; Total VGa = Bio VGa + Non bio VGa; Net REFa = Total VGa + Heat +  
683 Plastic board + Brick.

684

### 685 **3.5 Overall implications, limitations and perspectives**

686 SOC enhancement was shown as a relatively minor contributor to climate change  
687 mitigation, given the important effect of avoided petrochemical plastic production and use.  
688 However, it should be highlighted that the SOC level simulated after three rotations (ca. 134000  
689 kg ha<sup>-1</sup>) is significantly higher than the average SOC in French lands covered by grass or forest  
690 (81000- 85000 kg ha<sup>-1</sup>, Pellerin et al., 2021), and well above the 41000 kg ha<sup>-1</sup> observed after  
691 105 years of the initial vegetation system. Nevertheless, SOC deserves more attention and  
692 experimental investigation in real conditions in order to validate the simulation results. Such  
693 experiments will, in contrast to the simulation approach, require many years.

694 Combining the simulation results for the SOC, biomass growth, decay, and amount of  
695 products allows calculating the total C stock and comparing it to the C from CO<sub>2</sub> captured  
696 during the whole period (Fig. 11). The difference between stocks and captures represents the  
697 biogenic C released into the atmosphere (as CO<sub>2</sub> and CH<sub>4</sub>). The C stock in products is higher  
698 than in soil. The net stock represents the negative emissions that the BL scenario could induce  
699 (81%, 39%, 15% of total captured C, in the year 2050, 2100, 2290 respectively. Fig. s11 in SM).

700 Annualizing the CO<sub>2</sub> absorption to compare with annual grass, black locust could  
701 capture twice the amount captured by the initial vegetation, similar to a vigorous energy grass  
702 (Hamelin et al., 2012). Compared to 14 wood species cultivated in France (Albers et al., 2019a),  
703 black locust could fix more C than the average of these species over the same period while  
704 attaining maturity well before the average maturity time of about 80 years.

705

706 Fig. 11 Carbon captured over the cultivation period, and biogenic carbon stocks during the  
707 lifetime of the BL scenario.  
708

709 In the value chain proposed, bio-based products can replace fossil-based products with  
710 problematic environmental footprint at the level of their manufacturing and, significantly, of  
711 their end-of-life management.

712 The static LCA highlighted that replacing the initial vegetation with the black locust  
713 value chain is beneficial for the environment in 13 out of 16 environmental impacts (Table 1,  
714 italic fonts), mainly due to the fossil-based replacement. The use of resins/plastics in both bio-  
715 based and fossil-based products is critical in many impacts as highlighted by the LCA and  
716 confirmed by other studies (e.g., Nakano et al., 2018, Silva et al., 2013, etc.), therefore less or  
717 no resin additive is matter of investigation (Kouchaki-Penchah et al., 2016; Puettmann et al.,  
718 2016). The high environmental impacts of plastic production could be mitigated by other  
719 choices for the board material, as highlighted by the sensitivity analysis (SM section 5). Further,  
720 with the development of plastic recycling and replacement, less GHG emissions could be  
721 expected from production and incineration (Deng, 2014; Schwarz et al., 2021; Ye et al., 2017).

722 All conducted LCA modeling approaches indicate that the black locust system is  
723 generally better than the initial situation, either by measuring the consequence of this  
724 replacement as negative kg CO<sub>2</sub>-eq and negative net GMTC, or by measuring/comparing the  
725 actual impact. BLa scenario could be a negative emission strategy in the near- and mid-term  
726 (2030-2063) when net GMTC is negative. It is certainly a mitigation solution from 2026- 2029,  
727 when the net GMTC is lower than that of REFa system but still positive (Fig. 10). The black  
728 locust system alone satisfies the neutrality in this decade (2027), but its implementation requires  
729 producing feedstock and oil elsewhere, hence attention must be paid to the net GMTC of the  
730 whole BLa system. Its increase in the second half of the century could be mitigated with

731 appropriate solutions at the level of all manufacturing and end-of-life technologies, i.e. less  
732 fossil-based background processes and promoting wood material recycling instead of  
733 incineration. If the systems are scaled-up to the whole CV-lands in France, the REFa system  
734 increases the global mean temperature with 0.0020°C and 0.00576C by 2050 and 2100. BLa  
735 system decreases the temperature with 0.0006°C in the mid-term, but increases it by 2100 with  
736 0.0002°C, with a peak in between which must be mitigated. Of course, these values are only  
737 orders of magnitude, to be relativized to the feasibility of using the whole CV-land potential.

738

#### 739 **4 Conclusions**

740 This study investigated the relevance of using black locust as biopump to contribute to  
741 global warming mitigation following the CSAAP concept. A value chain was proposed from  
742 tree planting on CV-lands in France, to bio-based products manufacturing, use, and end of life,  
743 as an alternative to leaving the CV-lands as they are presently. This system runs from the first  
744 year of cultivation to the end of three rotations and to the end-of-life of the last product produced  
745 from biomass, encompassing 267 years.

746 Simulation results of biomass growth, decay, and SOC changes showed, throughout  
747 three rotations, that the black locust system induces more C stock in soils (considered as  
748 negative emission) than the initial vegetation, for an annual average SOC increase of 21%. This  
749 also applies with regards to the C stored in the biomass of both systems. It was found that 15%  
750 of the carbon captured by 3 rotations of black locust is still stocked in technosphere after 260  
751 years.

752 Replacing the initial vegetation with the black locust value chain was shown to mitigate  
753 global warming and was highlighted as beneficial to the environment for 13 of the 16 impact  
754 categories evaluated through consequential LCA. Hence, improving climate change was shown  
755 to result in minor trade-offs with the other environmental impacts. It should be noted that

756 avoided plastic, associated to the secondary product MDF, is key to climate change impact and  
757 to the performance of most other impacts.

758         Considering the climate goals, black locust value chain implementation results in  
759 climate cooling effect by net negative emissions, in the near and mid-term, but with a GMTC  
760 overshoot (BLa) observed from the second half of the century, which must be mitigated. SOC  
761 has little contribution to carbon storage. Therefore, this study highlighted the importance of  
762 acting on emissions stemming from manufacturing and end-of-life (all background processes),  
763 which offset the benefit of C capture to achieve the goal of neutrality.

764         The dynamic approach used for global warming evaluation clearly shows that the  
765 mitigation potential is relative to the time scale. Approaching the end-of-life of the system  
766 results in emissions from land use change (if black locust is no more cultivated), and from the  
767 end-of-life management of the products, leading to the C stocks depletion and C emissions.  
768 Therefore, if such a strategy is implemented in reality, a continuous assessment of the carbon  
769 flows and other GHG is necessary, together with adapted solutions (e.g. recycling instead of  
770 landfilling, technologies with no emissions, etc.) to preserve the climate benefit.

771         Finally, these results highlight the benefit of using biopump for applying the CSAAP  
772 concept in mitigating climate change and other environmental impacts, providing the scientific  
773 basis for policy makers. However, there are some limitations that deserve further investigations.  
774 The carbon balance at the level of plant cultivation should be confirmed by experiments or  
775 specific investigation for each CV-land locally. In the practical applications, the land use cannot  
776 be guaranteed for such a long time, and the mono cultivation of one specie is unrealistic.  
777 Moreover, if all the available CV land in France were used for the planting of black locust and  
778 if all the wood were used only for the proposed products, the production would far exceed the  
779 market. Indeed, with the development of technology and market, there will be more and more

780 bio-based products instead of petrochemical materials, and the marginal products substituted in  
781 the consequential LCA will be challenged.

782 This study provided an integrated and comprehensive framework for proposing and  
783 analyzing mitigation solutions for global warming, which could be applied to other cases. Other  
784 combinations biopump/bio-based product could be analyzed; it is also possible to propose a  
785 panel of combined solutions with different plants and products for a given region.

786

## 787 **Acknowledgments**

788 This work was carried out within the research project Cambioscop  
789 (<https://cambioscop.cnrs.fr>), financed by the French National Research Agency, Programme  
790 Investissement d'Avenir (ANR-17-MGPA-0006) and Region Occitanie (18015981).  
791 Additional funding was supplied by the Chinese Scholarship Council (201801810082).

792

## 793 **Supplementary material**

794 Supplementary document contains : documented LCA inventory, details on modeling  
795 approaches, results.

796

## 797 **References**

798 Adamopoulos, S., Passialis, C., Voulgaridis, E., 2007. Strength properties of juvenile and  
799 mature wood in black locust (*Robinia pseudoacacia* L.). *Wood Fiber Sci.* 39, 241–249.  
800 ADEME, 2018. Updated Energy-Climate Scenario ADEME 2035-2050.  
801 Albers, A., Collet, P., Benoist, A., Hélias, A., 2019a. Data and non-linear models for the  
802 estimation of biomass growth and carbon fixation in managed forests. *Data Br.* 23.  
803 <https://doi.org/10.1016/j.dib.2019.103841>

804 Albers, A., Collet, P., Lorne, D., Benoist, A., Hélias, A., 2019b. Coupling partial-equilibrium  
805 and dynamic biogenic carbon models to assess future transport scenarios in France.  
806 *Appl. Energy* 239, 316–330. <https://doi.org/10.1016/j.apenergy.2019.01.186>

807 Andrade, C., Ranguel, A. De, Zamora-ledezma, E., Hamelin, L., 2022. A review on the  
808 interplay between bioeconomy and soil organic carbon stocks maintenance .

809 Barna, L.T., 2021. A climate goal – based , multicriteria method for system evaluation in life  
810 cycle assessment. *Int. J. Life Cycle Assess.* <https://doi.org/10.1007/s11367-021-01991-1>

811 Brandao, M., Martin, M., Cowie, A., Hamelin, L., Zamagni, A., 2017. Consequential Life  
812 Cycle Assessment: What, How, and Why? *Encycl. Sustain. Technol.* 1, 277–284.  
813 <https://doi.org/10.1016/B978-0-12-409548-9.10068-5>

814 Cadorel, X., Crawford, R., 2019. Life cycle analysis of cross laminated timber in buildings: a  
815 review. *Engag. Archit. Sci. Meet. Challenges High. Density 52nd Int. Conf. Archit. Sci.*  
816 *Assoc.* 2018 15978, 107–114.

817 Cardellini, G., Mutel, C.L., Vial, E., Muys, B., 2018. Temporalis, a generic method and tool  
818 for dynamic Life Cycle Assessment. *Sci. Total Environ.* 645, 585–595.  
819 <https://doi.org/10.1016/j.scitotenv.2018.07.044>

820 Chen, C.X., Pierobon, F., Ganguly, I., 2019. Life Cycle Assessment (LCA) of Cross-  
821 Laminated Timber (CLT) produced in Western Washington: The role of logistics and  
822 wood species mix. *Sustain.* 11: <https://doi.org/10.3390/su11051278>

823 Chen, D., Rojas, M., Samset, B.H., Cobb, K., Diongue-Niang, A., Edwards, P., Emori, S.,  
824 Faria, S.H., Hawkins, E., Hope, P., Huybrechts, P., Meinshausen, M., Mustafa, S.K.,  
825 Plattner, G.-K., Treguier, A.M., 2021. Framing, Context, and Methods., in: *Climate*  
826 *Change 2021: The Physical Science Basis. Contribution of Working Group I to the*  
827 *Sixth Assessment Report of the Intergovernmental Panel on Climate Change. IPCC.*

828 Chen, J., Zhang, H., Zhang, X., Tang, M., 2020. Arbuscular mycorrhizal symbiosis mitigates  
829 oxidative injury in black locust under salt stress through modulating antioxidant defence  
830 of the plant. *Environ. Exp. Bot.* 175, 104034.  
831 <https://doi.org/10.1016/j.envexpbot.2020.104034>

832 Ciccarese, L., Pellegrino, P., Silli, V., Zanchi, G., 2014. Short rotation forestry and methods  
833 for carbon accounting. A case study of black locust (*Robinia pseudoacacia* L.) plantation  
834 in central Italy. *Rapporti* 200, 5.

835 Clivot, H., Mouny, J.C., Duparque, A., Dinh, J.L., Denoroy, P., Houot, S., Vertès, F.,  
836 Trochard, R., Bouthier, A., Sagot, S., Mary, B., 2019. Modeling soil organic carbon  
837 evolution in long-term arable experiments with AMG model. *Environ. Model. Softw.*  
838 118, 99–113. <https://doi.org/10.1016/j.envsoft.2019.04.004>

839 Cordier, S., Blanchet, P., Robichaud, F., Amor, B., 2022. Dynamic LCA of the increased use  
840 of wood in buildings and its consequences: Integration of CO<sub>2</sub> sequestration and  
841 material substitutions. *Build. Environ.* 226, 109695.  
842 <https://doi.org/10.1016/j.buildenv.2022.109695>

843 Corradini, G., Pierobon, F., Zanetti, M., 2019. Product environmental footprint of a cross-  
844 laminated timber system: a case study in Italy. *Int. J. Life Cycle Assess.* 24, 975–988.  
845 <https://doi.org/10.1007/s11367-018-1541-x>

846 Couret, L., Irle, M., Belloncle, C., Cathala, B., 2017. Extraction and characterization of  
847 cellulose nanocrystals from post-consumer wood fiberboard waste. *Cellulose* 24, 2125–  
848 2137. <https://doi.org/10.1007/s10570-017-1252-7>

849 Cowie, A.L., Berndes, G., Bentsen, N.S., Brandão, M., Cherubini, F., Egnell, G., George, B.,  
850 Gustavsson, L., Hanewinkel, M., Harris, Z.M., Johnsson, F., Junginger, M., Kline, K.L.,  
851 Koponen, K., Koppejan, J., Kraxner, F., Lamers, P., Majer, S., Marland, E., Nabuurs,  
852 G.J., Pelkmans, L., Sathre, R., Schaub, M., Smith, C.T., Soimakallio, S., Van Der Hilst,

853 F., Woods, J., Ximenes, F.A., 2021. Applying a science-based systems perspective to  
854 dispel misconceptions about climate effects of forest bioenergy. *GCB Bioenergy* 13,  
855 1210–1231. <https://doi.org/10.1111/gcbb.12844>

856 da Costa, T.P., Quinteiro, P., Tarelho, L.A. da C., Arroja, L., Dias, A.C., 2018. Environmental  
857 impacts of forest biomass-to-energy conversion technologies: Grate furnace vs. fluidised  
858 bed furnace. *J. Clean. Prod.* 171, 153–162. <https://doi.org/10.1016/j.jclepro.2017.09.287>

859 Deng, Y., 2014. Life cycle assessment of biobased fibre-reinforced polymer composites.  
860 World Scientific. [https://doi.org/10.1142/9789814566469\\_0063](https://doi.org/10.1142/9789814566469_0063)

861 Dodoo, A., Gustavsson, L., Sathre, R., 2014. Lifecycle primary energy analysis of low-energy  
862 timber building systems for multi-storey residential buildings. *Energy Build.* 81, 84–97.  
863 <https://doi.org/10.1016/j.enbuild.2014.06.003>

864 DRIAS CERFACS, IPSL, M.-F., 2013. CNRM-CERFACS-CM5/CNRM-ALADIN63-  
865 RCP4.5. DRIAS les Futur. du Clim.

866 ecoinvent, 2020. Ecoinvent 3.5 database [WWW Document]. URL  
867 [https://www.ecoinvent.org/database/ecoinvent-37/new-data-in-ecoinvent-37/new-data-](https://www.ecoinvent.org/database/ecoinvent-37/new-data-in-ecoinvent-37/new-data-in-ecoinvent-37.html)  
868 [in-ecoinvent-37.html](https://www.ecoinvent.org/database/ecoinvent-37/new-data-in-ecoinvent-37/new-data-in-ecoinvent-37.html)

869 European Commission-Joint Research Centre., 2010. General guide for life cycle  
870 assessment—detailed guidance. In: *ILCD Handbook—International Reference Life*  
871 *Cycle Data System*, first ed.

872 European Commission, 2021. EU Reference Scenario 2020 [WWW Document]. URL  
873 [https://energy.ec.europa.eu/data-and-analysis/energy-modelling/eu-reference-scenario-](https://energy.ec.europa.eu/data-and-analysis/energy-modelling/eu-reference-scenario-2020_en)  
874 [2020\\_en](https://energy.ec.europa.eu/data-and-analysis/energy-modelling/eu-reference-scenario-2020_en)

875 Fazio, S., Biganzioli, F., De Laurentiis, V., Zampori, L., Sala, S., Diaconu, E., 2018a.  
876 Supporting information to the characterisation factors of recommended EF Life Cycle  
877 Impact Assessment methods, version 2, from ILCD to EF 3.0, EUR 29600 EN, European

878 Commission, Ispra, 2018, ISBN 978-92-79-98584-3, doi:10.2760/002447, PUBSY No.  
879 JRC114822., New Models and Differences with ILCD, EUR.  
880 <https://doi.org/10.2760/002447>

881 Fazio, S., Zampori, L., A, D.S., Kusche, O., 2018b. Guide on Life Cycle Inventory (LCI) data  
882 generation for the Environmental Footprint. <https://doi.org/10.2760/745658>

883 Food and Agriculture Organization of the United Nations, 2020. GSOCmap v1.5.0 [WWW  
884 Document]. URL <http://54.229.242.119/GSOCmap/>

885 González-García, S., Gasol, C.M., Moreira, M.T., Gabarrell, X., Pons, J.R.I., Feijoo, G.,  
886 2011. Environmental assessment of black locust (*Robinia pseudoacacia* L.)-based  
887 ethanol as potential transport fuel. *Int. J. Life Cycle Assess.* 16, 465–477.  
888 <https://doi.org/10.1007/s11367-011-0272-z>

889 Göswein, V., Pittau, F., Silvestre, J.D., Freire, F., Habert, G., 2020. Dynamic life cycle  
890 assessment of straw-based renovation: A case study from a Portuguese neighbourhood.  
891 *IOP Conf. Ser. Earth Environ. Sci.* 588. <https://doi.org/10.1088/1755-1315/588/4/042054>

892 Guest, G., Cherubini, F., Strømman, A.H., 2013. Global Warming Potential of Carbon  
893 Dioxide Emissions from Biomass Stored in the Anthroposphere and Used for Bioenergy  
894 at End of Life. *J. Ind. Ecol.* 17, 20–30. <https://doi.org/10.1111/j.1530-9290.2012.00507.x>

895 Guo, H., Liu, Y., Meng, Y., Huang, H., Sun, C., Shao, Y., 2017. A Comparison of the energy  
896 saving and carbon reduction performance between reinforced concrete and cross-  
897 laminated timber structures in residential buildings in the severe cold region of China.  
898 *Sustain.* 9. <https://doi.org/10.3390/su9081426>

899 Hamelin, L., Jørgensen, U., Petersen, B.M., Olesen, J.E., Wenzel, H., 2012. Modelling the  
900 carbon and nitrogen balances of direct land use changes from energy crops in Denmark:  
901 A consequential life cycle inventory. *GCB Bioenergy* 4, 889–907.  
902 <https://doi.org/10.1111/j.1757-1707.2012.01174.x>

903 Hansen, J.H., Hamelin, L., Taghizadeh-Toosi, A., Olesen, J.E., Wenzel, H., 2020.  
904 Agricultural residues bioenergy potential that sustain soil carbon depends on energy  
905 conversion pathways. *GCB Bioenergy* 12, 1002–1013.  
906 <https://doi.org/10.1111/gcbb.12733>

907 IPCC, 2019. Refinement to the 2006 IPCC Guidelines for National Greenhouse Gas  
908 Inventories Volume 5 Waste, IPCC Good Practice Guidance and Uncertainty  
909 Management in National Greenhouse Gase Inventories.

910 ISO, 2006a. Environmental management: life cycle assessment; Principles and Framework.  
911 ISO.

912 ISO, 2006b. Environmental management: life cycle assessment; requirements and guidelines.  
913 ISO Geneva, Switzerland.

914 Jayalath, A., Navaratnam, S., Ngo, T., Mendis, P., Hewson, N., Aye, L., 2020. Life cycle  
915 performance of Cross Laminated Timber mid-rise residential buildings in Australia.  
916 *Energy Build.* 223, 110091. <https://doi.org/10.1016/j.enbuild.2020.110091>

917 Kassara, G., Pena Verrier, G., Chammas, M., Fournie, L., Mainsant, A., Marchal, D.,  
918 Parrouffe, J.-M., 2019. Trajectories of evolution of the electricity mix 2020-2060:  
919 Additional analyses, FAQs, Report on data.

920 Keel, S.G., Leifeld, J., Mayer, J., Taghizadeh-Toosi, A., Olesen, J.E., 2017. Large uncertainty  
921 in soil carbon modelling related to method of calculation of plant carbon input in  
922 agricultural systems. *Eur. J. Soil Sci.* 68, 953–963. <https://doi.org/10.1111/ejss.12454>

923 Keresztesi, B., 1983. Breeding and cultivation of black locust, *Robinia pseudoacacia*, in  
924 Hungary. *For. Ecol. Manage.* 6, 217–244. [https://doi.org/10.1016/S0378-1127\(83\)80004-](https://doi.org/10.1016/S0378-1127(83)80004-8)  
925 8

926 Kouchaki-Penchah, H., Sharifi, M., Mousazadeh, H., Zarea-Hosseiniabadi, H., 2016. Life  
927 cycle assessment of medium-density fiberboard manufacturing process in Islamic

928 Republic of Iran. *J. Clean. Prod.* 112, 351–358.  
929 <https://doi.org/10.1016/j.jclepro.2015.07.049>

930 Lan, K., Kelley, S.S., Nepal, P., Yao, Y., 2020. Dynamic life cycle carbon and energy  
931 analysis for cross-laminated timber in the Southeastern United States. *Environ. Res. Lett.*  
932 15, 124036. <https://doi.org/10.1088/1748-9326/abc5e6>

933 Launay, C., Constantin, J., Chlebowski, F., Houot, S., Graux, A.I., Klumpp, K., Martin, R.,  
934 Mary, B., Pellerin, S., Therond, O., 2021. Estimating the carbon storage potential and  
935 greenhouse gas emissions of French arable cropland using high-resolution modeling.  
936 *Glob. Chang. Biol.* 27, 1645–1661. <https://doi.org/10.1111/gcb.15512>

937 Minasny, B., Malone, B.P., McBratney, A.B., Angers, D.A., Arrouays, D., Chambers, A.,  
938 Chaplot, V., Chen, Z.S., Cheng, K., Das, B.S., Field, D.J., Gimona, A., Hedley, C.B.,  
939 Hong, S.Y., Mandal, B., Marchant, B.P., Martin, M., McConkey, B.G., Mulder, V.L.,  
940 O'Rourke, S., Richer-de-Forges, A.C., Odeh, I., Padarian, J., Paustian, K., Pan, G.,  
941 Poggio, L., Savin, I., Stolbovoy, V., Stockmann, U., Sulaeman, Y., Tsui, C.C., Vågen,  
942 T.G., van Wesemael, B., Winowiecki, L., 2017. Soil carbon 4 per mille. *Geoderma* 292,  
943 59–86. <https://doi.org/10.1016/j.geoderma.2017.01.002>

944 Nakano, K., Ando, K., Takigawa, M., Hattori, N., 2018. Life cycle assessment of wood-based  
945 boards produced in Japan and impact of formaldehyde emissions during the use stage.  
946 *Int. J. Life Cycle Assess.* 23, 957–969. <https://doi.org/10.1007/s11367-017-1343-6>

947 Negishi, K., Lebert, A., Almeida D., Chevalier J., Tiruta-Barna, L., 2019, Evaluating climate  
948 change pathways through a building's lifecycle based on Dynamic Life Cycle  
949 Assessment, *Building and Environment*, 164, 2019, 106377

950 Nicolescu, V.N., Hernea, C., Bakti, B., Keserű, Z., Antal, B., Rédei, K., 2018. Black locust  
951 (*Robinia pseudoacacia* L.) as a multi-purpose tree species in Hungary and Romania: a  
952 review. *J. For. Res.* 29, 1449–1463. <https://doi.org/10.1007/s11676-018-0626-5>

953 Nicolescu, V.N., Rédei, K., Mason, W.L., Vor, T., Pöetzelsberger, E., Bastien, J.C., Brus, R.,  
954 Benčať, T., Đodan, M., Cvjetkovic, B., Andrašev, S., La Porta, N., Lavnyy, V.,  
955 Mandžukovski, D., Petkova, K., Roženbergar, D., Wąsik, R., Mohren, G.M.J.,  
956 Monteverdi, M.C., Musch, B., Klisz, M., Perić, S., Keça, L., Bartlett, D., Hernea, C.,  
957 Pástor, M., 2020. Ecology, growth and management of black locust (*Robinia*  
958 *pseudoacacia* L.), a non-native species integrated into European forests. *J. For. Res.* 31,  
959 1081–1101. <https://doi.org/10.1007/s11676-020-01116-8>

960 Onyeaju, M.C., Osarolube, E., Chukwuocha, E.O., Ekuma, C.E., Omasheye, G.A.J., 2012.  
961 Comparison of the Thermal Properties of Asbestos and Polyvinylchloride (PVC) Ceiling  
962 Sheets. *Mater. Sci. Appl.* 03, 240–244. <https://doi.org/10.4236/msa.2012.34035>

963 Pehme, S., Veromann, E., Hamelin, L., 2017. Environmental performance of manure co-  
964 digestion with natural and cultivated grass – A consequential life cycle assessment. *J.*  
965 *Clean. Prod.* 162, 1135–1143. <https://doi.org/10.1016/j.jclepro.2017.06.067>

966 Pellerin, S., Bamière, L., Savini, I., Réchauchère, O., 2021. Stocker du carbone dans les sols  
967 français. Quel potentiel au regard de l’objectif 4 pour 1000 et à quel coût? *Stock. du*  
968 *carbone dans les sols français.* <https://doi.org/10.35690/978-2-7592-3149-2>

969 Petersen, B.M., Berntsen, J., Hansen, S., Jensen, L.S., 2005. CN-SIM - A model for the  
970 turnover of soil organic matter. I. Long-term carbon and radiocarbon development. *Soil*  
971 *Biol. Biochem.* 37, 359–374. <https://doi.org/10.1016/j.soilbio.2004.08.006>

972 Petersen, B.M., Knudsen, M.T., Hermansen, J.E., Halberg, N., 2013. An approach to include  
973 soil carbon changes in life cycle assessments. *J. Clean. Prod.* 52, 217–224.  
974 <https://doi.org/10.1016/j.jclepro.2013.03.007>

975 Piekarski, C.M., de Francisco, A.C., da Luz, L.M., Kovalski, J.L., Silva, D.A.L., 2017. Life  
976 cycle assessment of medium-density fiberboard (MDF) manufacturing process in Brazil.  
977 *Sci. Total Environ.* 575, 103–111. <https://doi.org/10.1016/j.scitotenv.2016.10.007>

978 Puettmann, M., Bergman, R., Oneil, E., 2016. Cradle to gate life cycle assessment of north  
979 American cellulosic fiberboard production. CORRIM Final Report. Univ. Washington.  
980 Seattle, WA. January 2016. 66 p. 1–66.

981 Rédei, K., Csiha, I., KeserU, Z., Gál, J., 2012. Influence of regeneration method on the yield  
982 and stem quality of black locust (*Robinia pseudoacacia* L.) Stands: A case study. *Acta*  
983 *Silv. Lignaria Hungarica* 8, 103–112. <https://doi.org/10.2478/v10303-012-0008-1>

984 Rédei, K., Csiha, I., Keseru, Z., Rásó, J., Kamandiné Végh, Á., Antal, B., 2014. Growth and  
985 Yield of Black Locust (*Robinia pseudoacacia* L.) Stands in Nyírség Growing Region  
986 (North-East Hungary). *South-east Eur. For.* 5, 13–22. [https://doi.org/10.15177/see-for.14-](https://doi.org/10.15177/see-for.14-04)  
987 04

988 Saez de Bikuña, K., Hamelin, L., Hauschild, M.Z., Pilegaard, K., Ibrom, A., 2018. A  
989 comparison of land use change accounting methods: seeking common grounds for key  
990 modeling choices in biofuel assessments. *J. Clean. Prod.* 177, 52–61.  
991 <https://doi.org/10.1016/j.jclepro.2017.12.180>

992 Sahoo, K., Bergman, R., Alanya-Rosenbaum, S., Gu, H., Liang, S., 2019. Life cycle  
993 assessment of forest-based products: A review. *Sustain.* 11, 1–30.  
994 <https://doi.org/10.3390/su11174722>

995 Schaubroeck, T., Schaubroeck, S., Heijungs, R., Zamagni, A., Brandão, M., Benetto, E.,  
996 2021. Attributional & consequential life cycle assessment: Definitions, conceptual  
997 characteristics and modelling restrictions. *Sustain.* 13.  
998 <https://doi.org/10.3390/su13137386>

999 Schwarz, A.E., Ligthart, T.N., Godoi Bizarro, D., De Wild, P., Vreugdenhil, B., van  
1000 Harmelen, T., 2021. Plastic recycling in a circular economy; determining environmental  
1001 performance through an LCA matrix model approach. *Waste Manag.* 121, 331–342.  
1002 <https://doi.org/10.1016/j.wasman.2020.12.020>

1003 Seserman, D.M., Pohle, I., Veste, M., Freese, D., 2018. Simulating climate change impacts on  
1004 hybrid-poplar and black locust short rotation coppices. *Forests* 9, 1–25.  
1005 <https://doi.org/10.3390/f9070419>

1006 Shen, Z., Tiruta-Barna, L., Hamelin, L., 2022a. From Hemp Grown on Carbon Vulnerable  
1007 Lands to Long-Lasting Bio-Based Products: Uncovering Trade-Offs between Overall  
1008 Environmental Impacts, Sequestration in Soils and Dynamic Influence on Global  
1009 Temperature. *Sequestration Soils Dyn. Influ. Glob. Temp.*

1010 Shen, Z., Tiruta-Barna, L., Karan S. K., Hamelin, L., 2022b, Simultaneous carbon storage in  
1011 arable land and anthropogenic products (CSAAP): Demonstrating an integrated concept  
1012 towards well below 2°C. *Resour. Conserv. Recycl.* 182, 106293.  
1013 <https://doi.org/10.1016/j.resconrec.2022.106293>

1014 Silva, D.A.L., Lahr, F.A.R., Garcia, R.P., Freire, F.M.C.S., Ometto, A.R., 2013. Life cycle  
1015 assessment of medium density particleboard (MDP) produced in Brazil. *Int. J. Life Cycle*  
1016 *Assess.* 18, 1404–1411. <https://doi.org/10.1007/s11367-013-0583-3>

1017 Silva, D.A.L., Lahr, F.A.R., Pavan, A.L.R., Saavedra, Y.M.B., Mendes, N.C., Sousa, S.R.,  
1018 Sanches, R., Ometto, A.R., 2014. Do wood-based panels made with agro-industrial  
1019 residues provide environmentally benign alternatives? An LCA case study of sugarcane  
1020 bagasse addition to particle board manufacturing. *Int. J. Life Cycle Assess.* 19, 1767–  
1021 1778. <https://doi.org/10.1007/s11367-014-0776-4>

1022 Stocker, T.F., Qin, D., Plattner, G.K., Tignor, M.M.B., Allen, S.K., Boschung, J., Nauels, A.,  
1023 Xia, Y., Bex, V., Midgley, P.M., 2013. Climate change 2013 the physical science basis:  
1024 Working Group I contribution to the fifth assessment report of the intergovernmental  
1025 panel on climate change. *Clim. Chang. 2013 Phys. Sci. Basis Work. Gr. I Contrib. to*  
1026 *Fifth Assess. Rep. Intergov. Panel Clim. Chang.* 9781107057, 1–1535.  
1027 <https://doi.org/10.1017/CBO9781107415324>

1028 Stone, K.R., 2009. *Robinia pseudoacacia*. In: Fire Effects Information System [WWW  
1029 Document]. U.S. Dep. Agric. For. Serv. Rocky Mt. Res. Station. Fire Sci. Lab. URL  
1030 <https://www.fs.fed.us/database/feis/plants/tree/robpse/all.html>

1031 Taghizadeh-Toosi, A., Glendining, M., Vejlin, J., Hutchings, N.J., Olesen, J.E., Christensen,  
1032 B.T., Kätterer, T., 2014. C-TOOL: A simple model for simulating whole-profile carbon  
1033 storage in temperate agricultural soils. *Ecol. Modell.* 292, 11–25.  
1034 <https://doi.org/10.1016/j.ecolmodel.2014.08.016>

1035 Takano, A., Hughes, M., Winter, S., 2014. A multidisciplinary approach to sustainable  
1036 building material selection: A case study in a Finnish context. *Build. Environ.* 82, 526–  
1037 535. <https://doi.org/10.1016/j.buildenv.2014.09.026>

1038 Tonini, D., Hamelin, L., Astrup, T.F., 2016. Environmental implications of the use of agro-  
1039 industrial residues for biorefineries: application of a deterministic model for indirect  
1040 land-use changes. *GCB Bioenergy* 8, 690–706. <https://doi.org/10.1111/gcbb.12290>

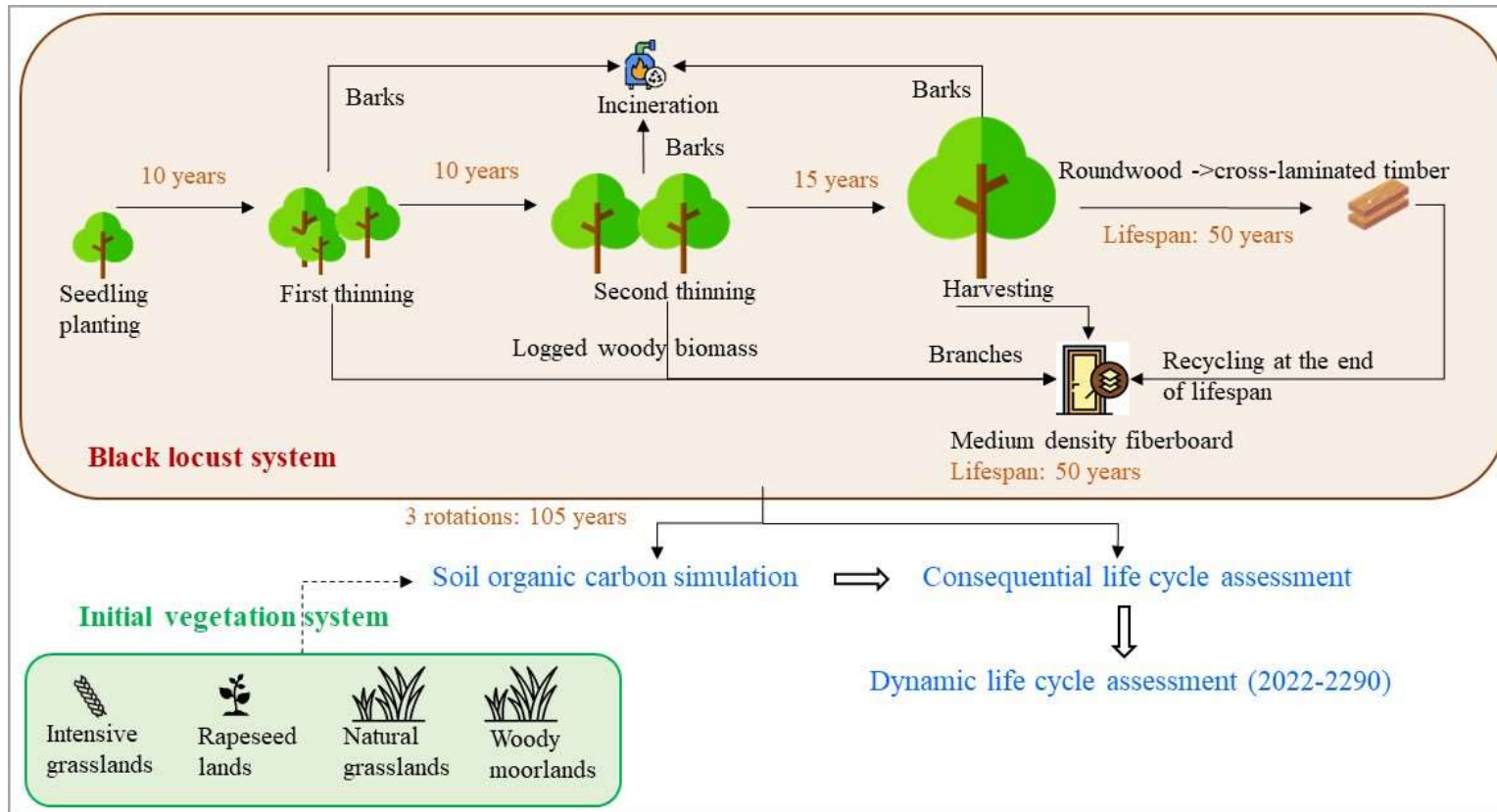
1041 Wang, B., Liu, G., Xue, S., 2012. Effect of black locust (*Robinia pseudoacacia*) on soil  
1042 chemical and microbiological properties in the eroded hilly area of China's loess plateau.  
1043 *Environ. Earth Sci.* 65, 597–607. <https://doi.org/10.1007/s12665-011-1107-8>

1044 Wang, J.J., Hu, C.X., Bai, J., Gong, C.M., 2015. Carbon sequestration of mature black locust  
1045 standson the loess plateau, China. *Plant, Soil Environ.* 61, 116–121.  
1046 <https://doi.org/10.17221/931/2014-PSE>

1047 Warne, A., 2016. Black locust (*Robinia pseudoacacia* L.). Best management practices in  
1048 Ontario, Ontario invasive plant council, Peterborough.

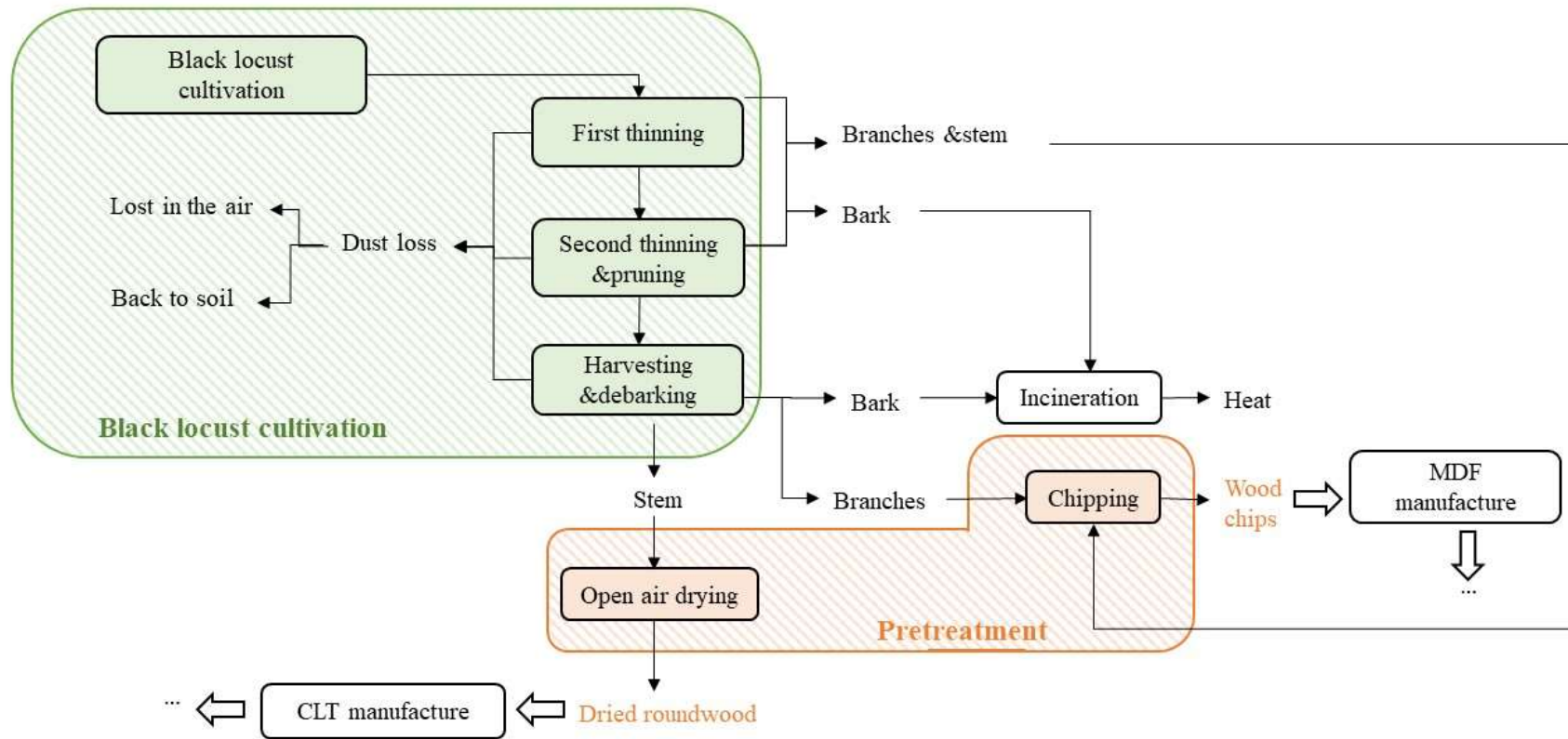
1049 Yang, Y., Tilman, D., 2020. Soil and root carbon storage is key to climate benefits of  
1050 bioenergy crops. *Biofuel Res. J.* 7, 1143–1148. <https://doi.org/10.18331/BRJ2020.7.2.2>

- 1051 Ye, L., Qi, C., Hong, J., Ma, X., 2017. Life cycle assessment of polyvinyl chloride production  
1052 and its recyclability in China. *J. Clean. Prod.* 142, 2965–2972.  
1053 <https://doi.org/10.1016/j.jclepro.2016.10.171>
- 1054 Yuan, Y., Guo, M., 2017. Do green wooden composites using lignin-based binder have  
1055 environmentally benign alternatives? A preliminary LCA case study in China. *Int. J. Life*  
1056 *Cycle Assess.* 22, 1318–1326. <https://doi.org/10.1007/s11367-016-1235-1>
- 1057 Żelazna, A., Kraszkiewicz, A., Przywara, A., Łagód, G., Suchorab, Z., Werle, S., Ballester, J.,  
1058 Nosek, R., 2019. Life cycle assessment of production of black locust logs and straw  
1059 pellets for energy purposes. *Environ. Prog. Sustain. Energy* 38, 163–170.  
1060 <https://doi.org/10.1002/ep.13043>
- 1061 Zieger, V., Lecompte, T., Hellouin de Menibus, A., 2020. Impact of GHGs temporal  
1062 dynamics on the GWP assessment of building materials: A case study on bio-based and  
1063 non-bio-based walls. *Build. Environ.* 185, 107210.  
1064 <https://doi.org/10.1016/j.buildenv.2020.107210>
- 1065
- 1066
- 1067



Graphical Abstract

(a) Black locust- cultivation, harvesting and pretreatment



(b) Black locust- MDF and CLT manufacture and disposal

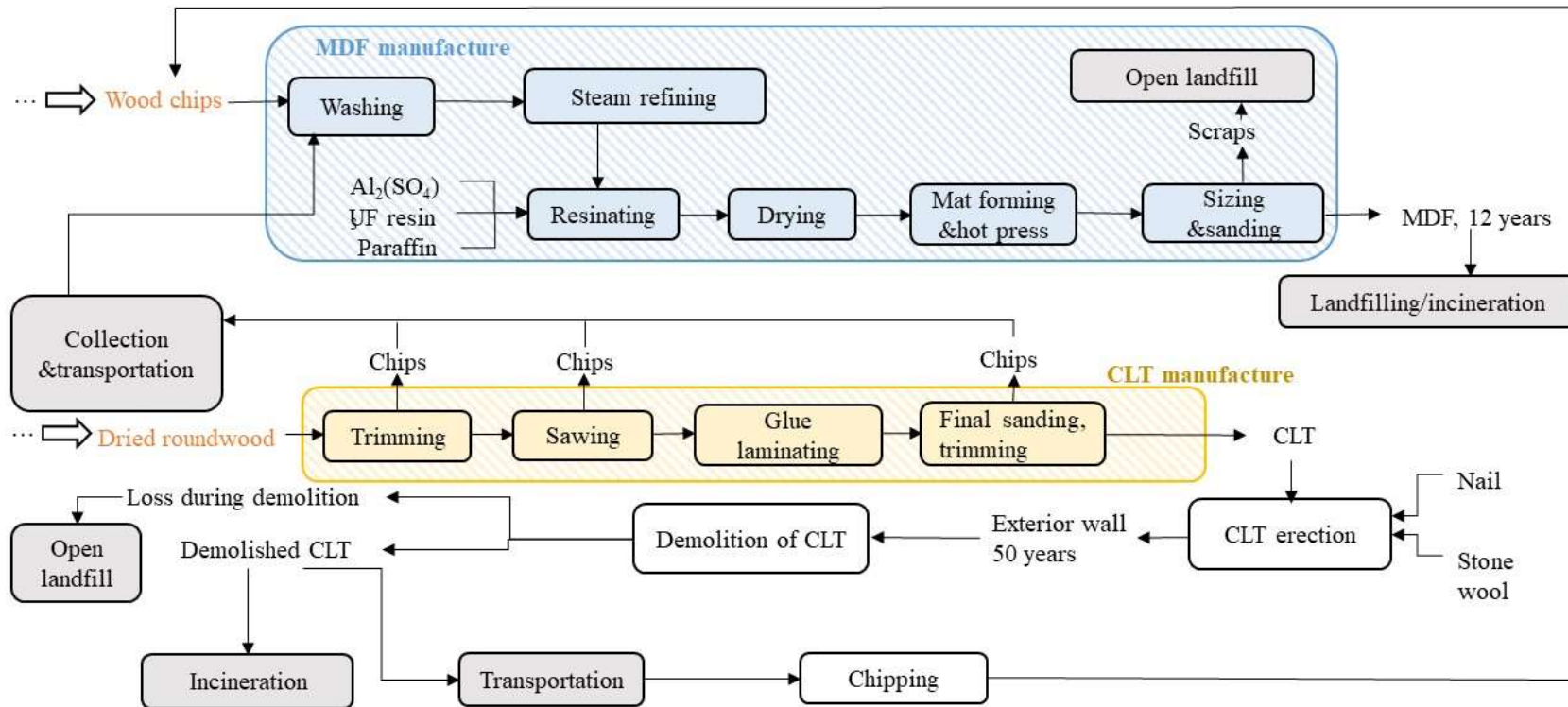


Fig. 1 Process flow diagram showing the key activities considered for (a) black locust cultivation, harvesting (green) and residual biomass management (orange), and (b) manufacture and disposal of cross-laminated timber (CLT; yellow) and medium density fiberboard (MDF; blue)

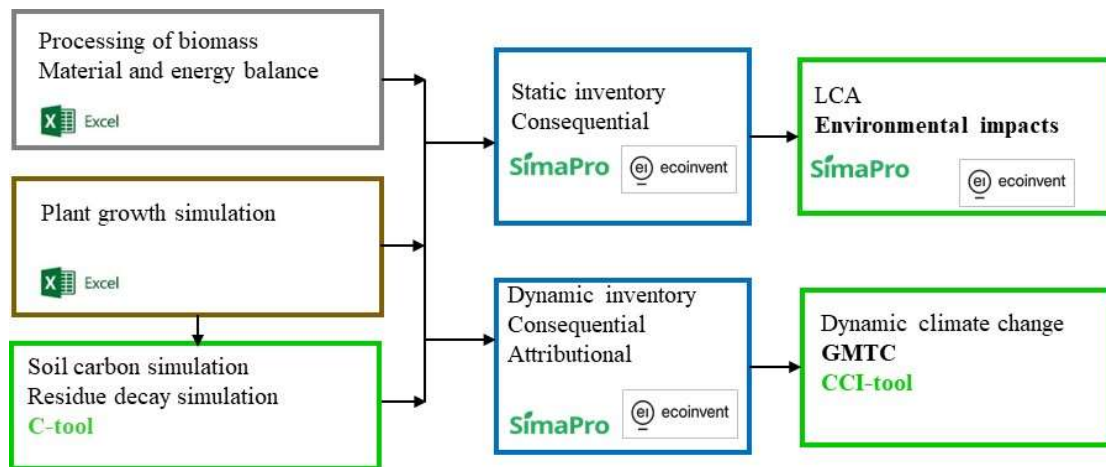


Fig. 2 Calculation steps followed in this study

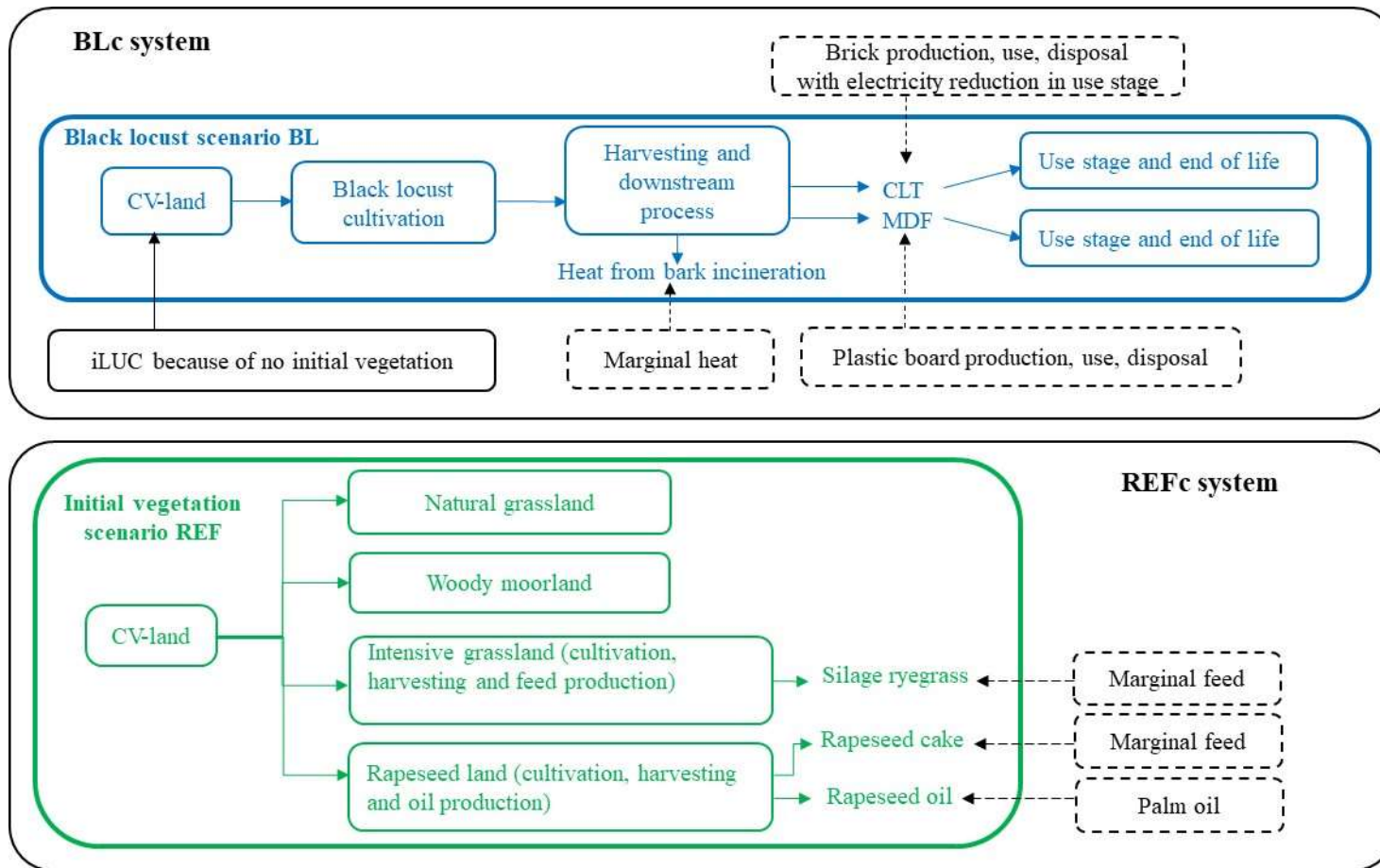


Fig. 3 System diagrams showing the boundaries considered in consequential LCA of business as usual (REFc) and black locust (BLc) systems, built on REF and BL scenarios respectively. CV-land: carbon vulnerable land; iLUC: Indirect land use changes; CLT: cross-laminated timber; MDF: medium density fiberboard. Full lines indicate induced processes while dotted lines represent avoided processes.

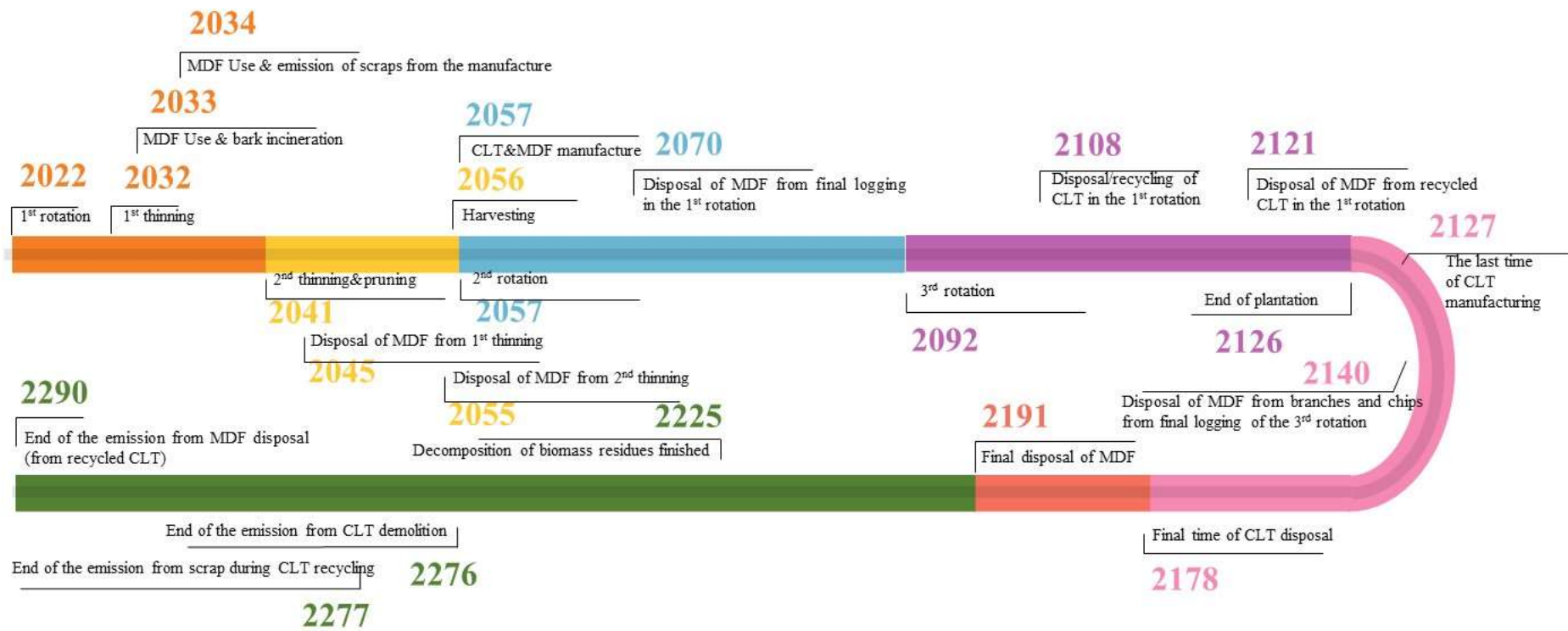


Fig. 4 Timeline of processes for dynamic LCA.

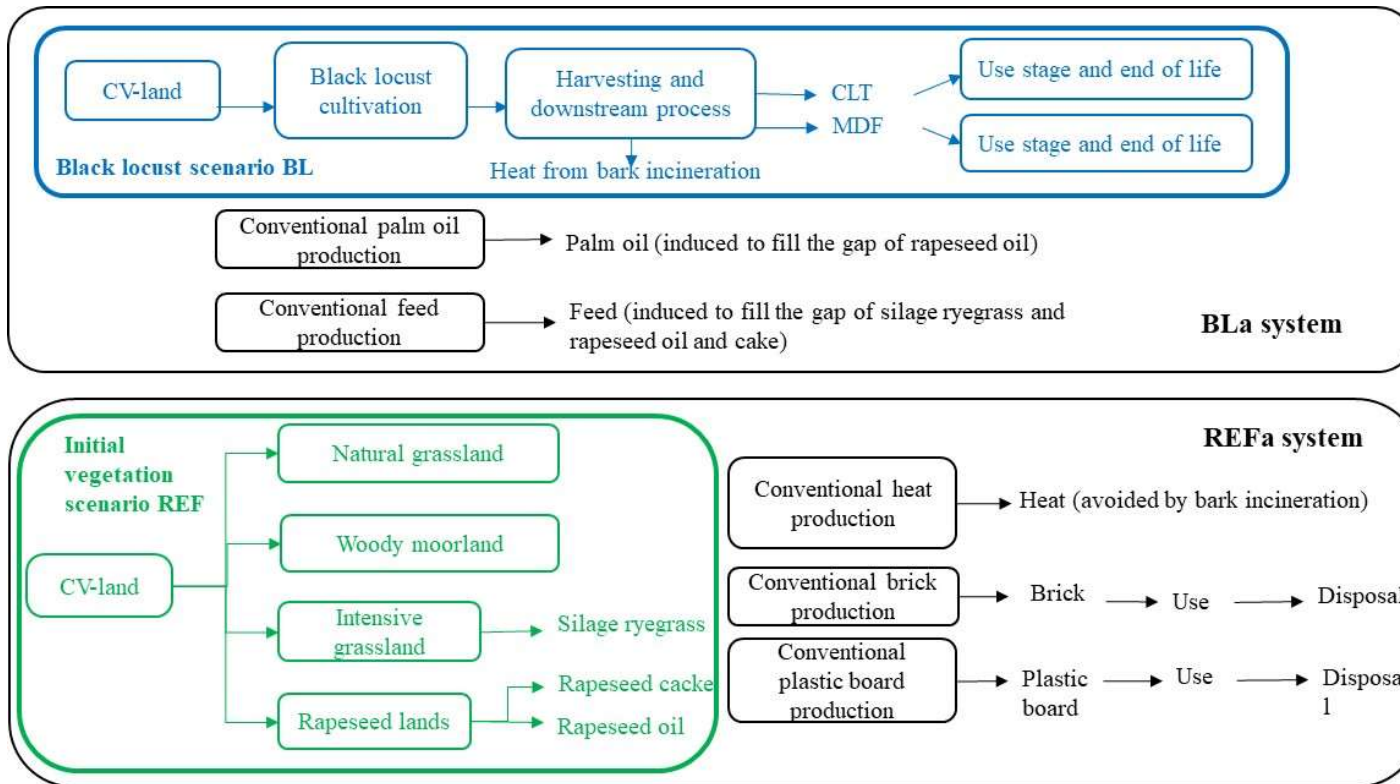


Fig. 5 System diagrams of business as usual (REFa) and black locust (BLa) systems, built on REF and BL scenarios respectively.

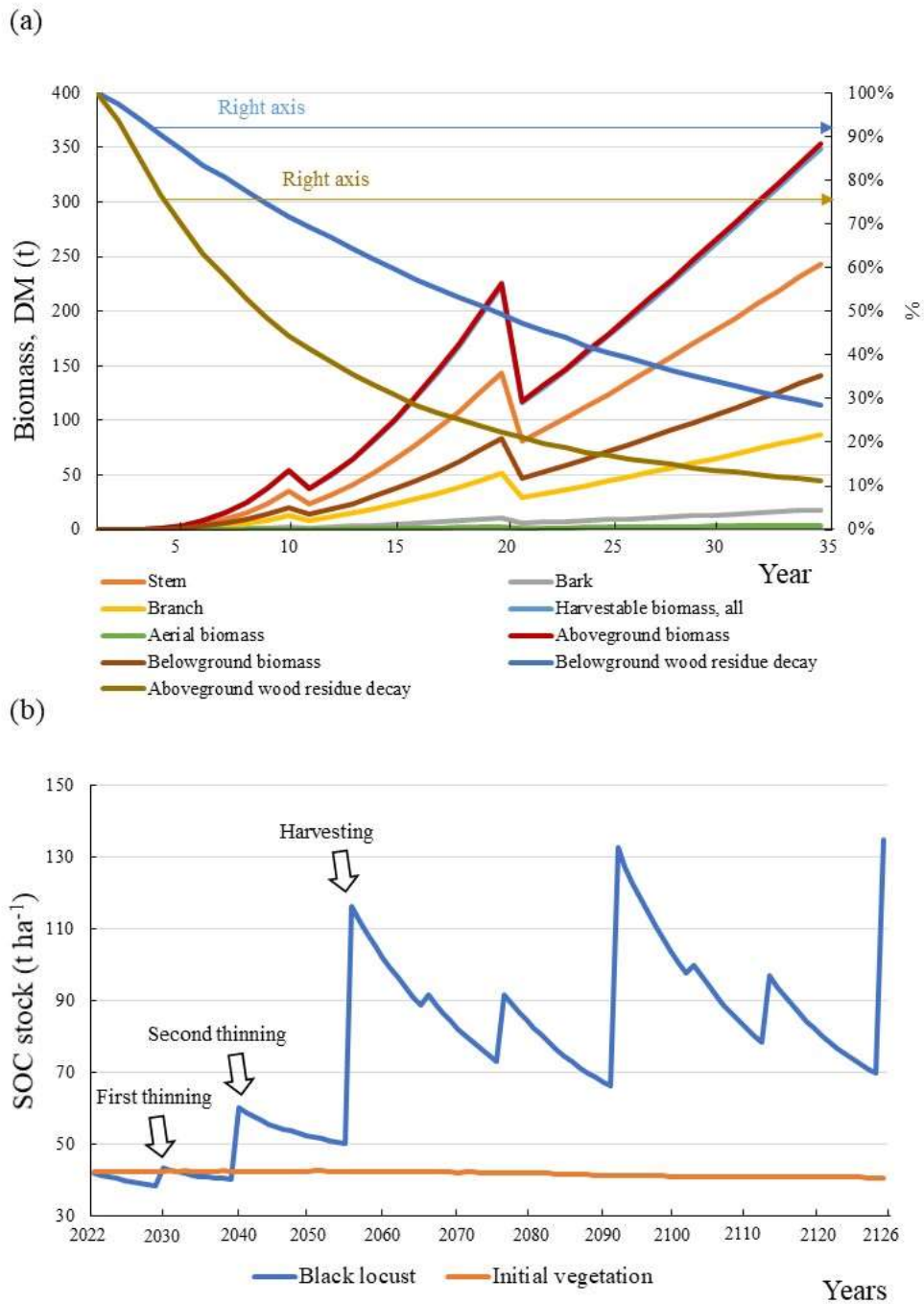


Fig. 6 Simulated (a) biomass growth and decay for black locust during one rotation, and (b) SOC evolution for black locust and initial vegetation during the cultivation period. Harvestable biomass: stem, branch and bark.

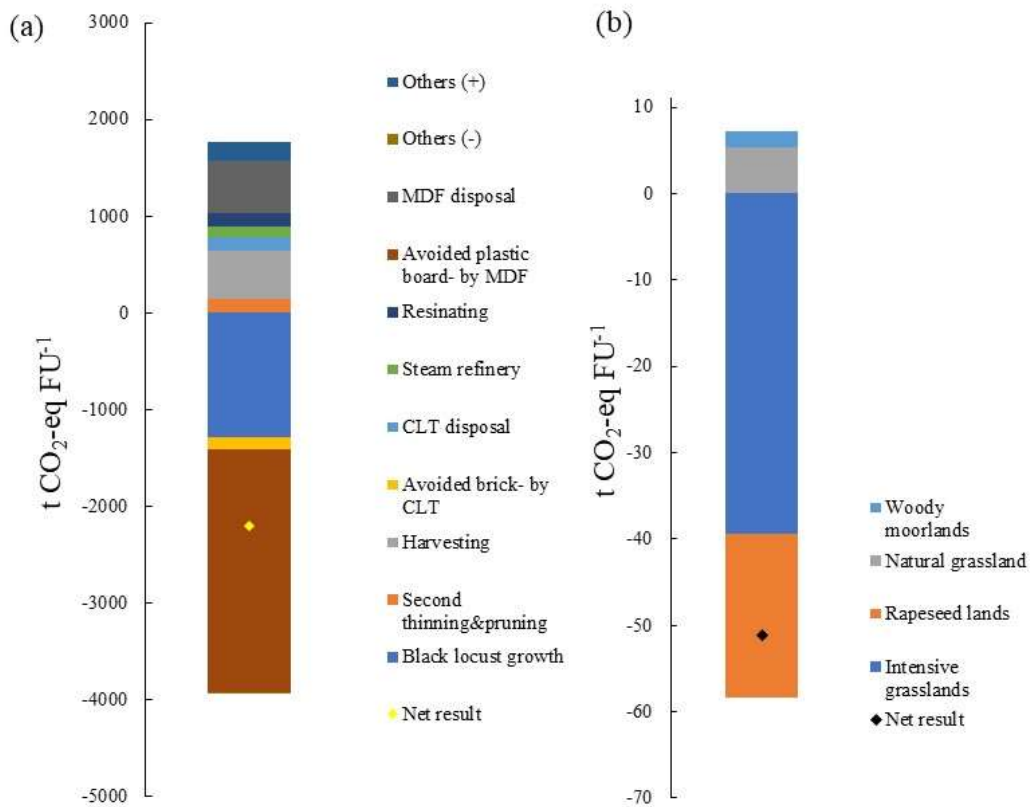


Fig.7 Climate change impact for (a) BLc and (b) REFc. Processes with contributions lower than 1% of the total impact (in absolute) were attributed to categories others (+) or (-) (Process contributions were computed as follows: e.g., process A has a contribution of 1 and process B of -1, then the contribution of process A is  $1/(abs(1)+abs(-1))=50\%$ ; details in SM). FU: functional unit.

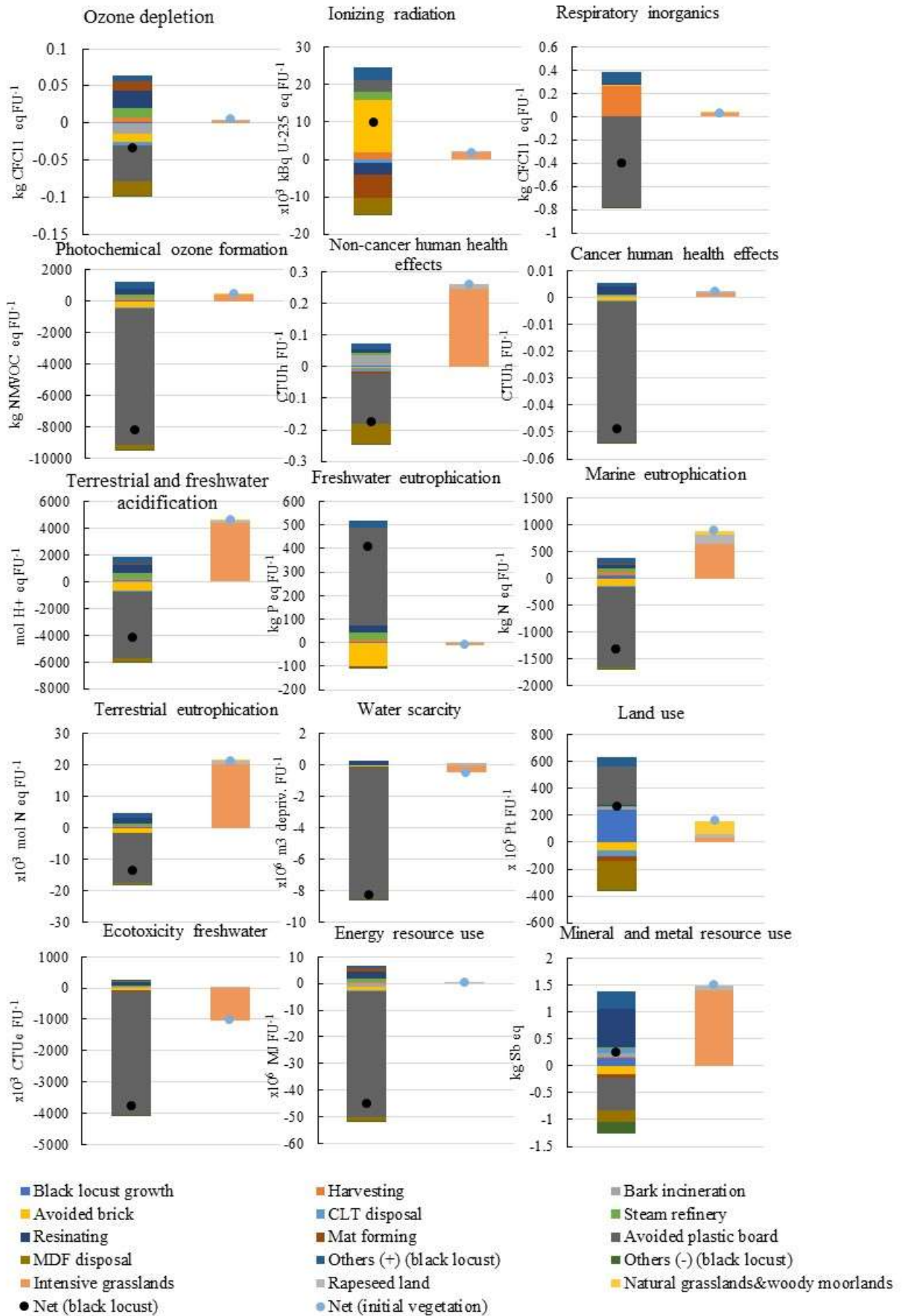


Fig. 8 LCA results for BLc (left bar) and REFc (right bar) scenarios for all impact categories of the EF method, with the exception of climate change impact.

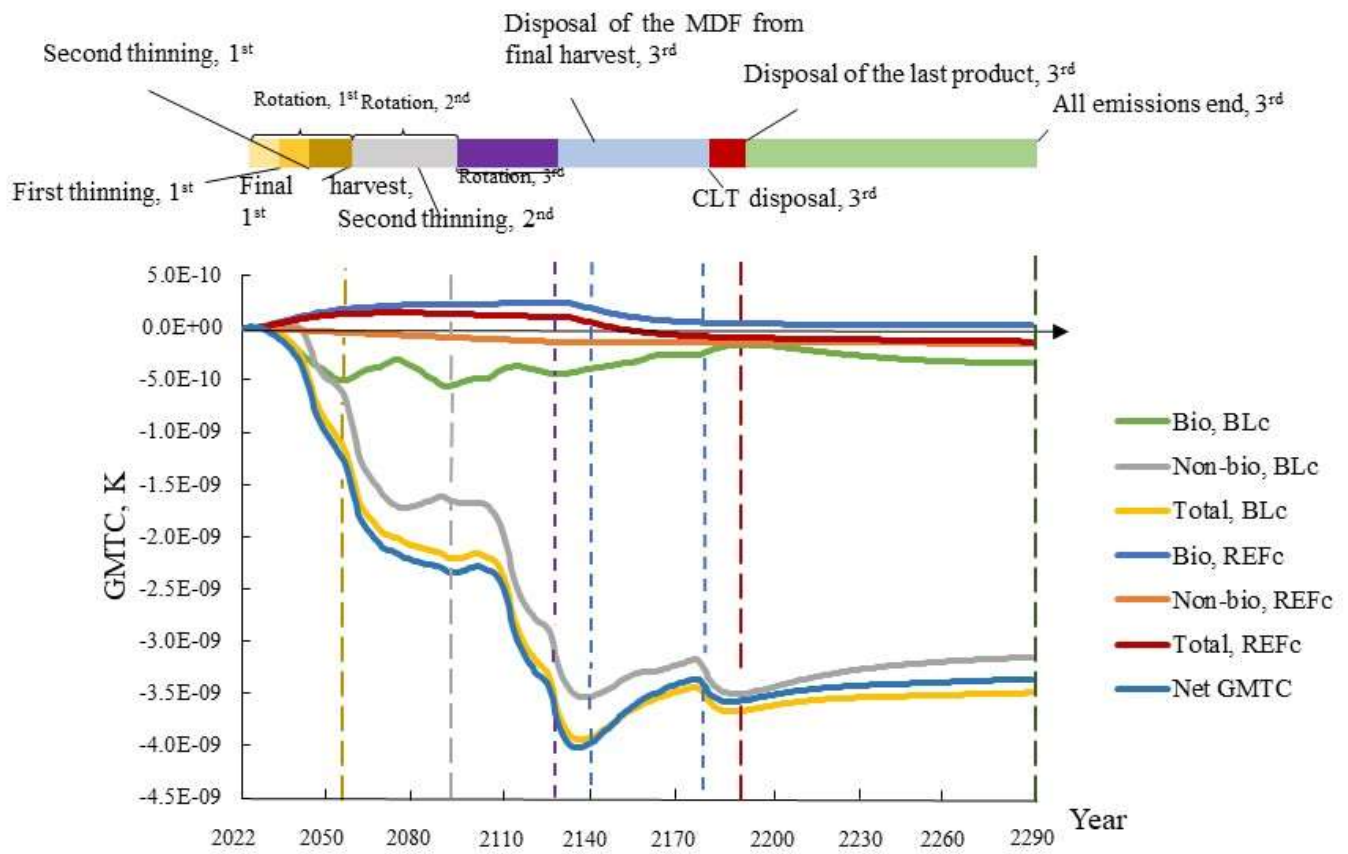


Fig. 9 GMTc results for all GHG sources from REFc and BLc scenarios, and the consequence of replacing REFc with BLc (Net GMTc). Total BLc = Bio BLc + Non bio BLc; Total REFc = Bio REFc + Non bio REFc; Net GMTc = Total BLc – Total REFc. 1<sup>st</sup>, 2<sup>nd</sup>, 3<sup>rd</sup> refer to the rotation number.

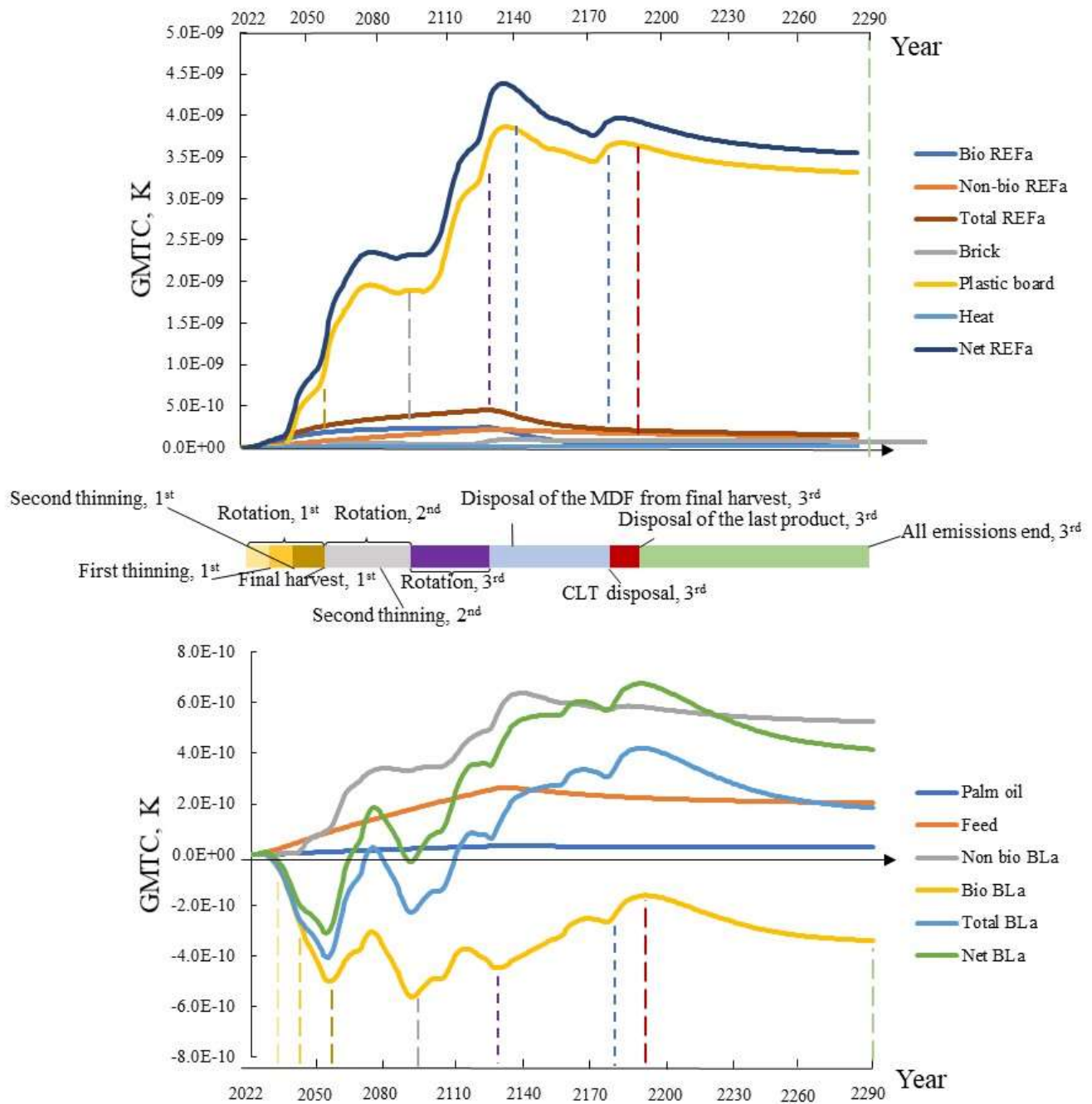


Fig. 10. GMTc evolution in REFa (above) and BLa (bottom) scenario with time. 1<sup>st</sup>, 2<sup>nd</sup>, 3<sup>rd</sup> refer to the rotation number. Total BLa = Bio BLa + Non bio BLa; Net BLa = Total BLa+ Palm oil + Feed; Total VGa = Bio VGa + Non bio VGa; Net REFa = Total VGa + Heat + Plastic board + Brick.

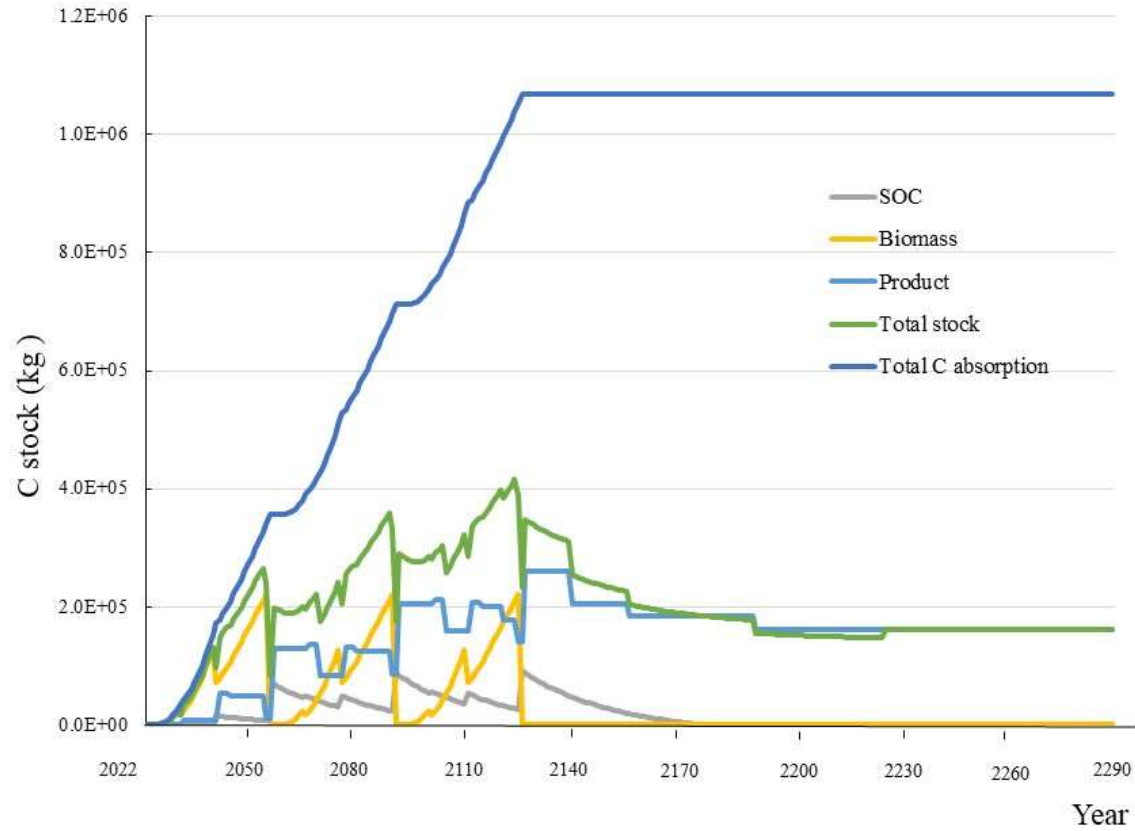


Fig. 11 Carbon captured over the cultivation period, and biogenic carbon stocks during the lifetime of the BL scenario.